Latin American Journal of Solids and Structures
www.lajss.org

Reflection of attenuated waves at the surface of a fractured porous solid saturated with two immiscible viscous fluids

Abstract

The mathematical model for wave motion in a fractured porous solid is solved for the propagation of harmonic plane wave along a general direction in 3-D space. The solution is obtained in the form of Christoffel equations, which are solved further to define the complex velocities and polarisations of five attenuated waves in the medium. Four of these waves are longitudinal waves and the one is transverse wave. For any of these five attenuated waves, a general inhomogeneous propagation is considered with a complex specification of slowness vector involving a finite non-dimensional inhomogeneity parameter. The phase velocities and attenuation coefficients are calculated for the inhomogeneous propagation of each of the five attenuated waves in the medium. A numerical example is studies to analyse the effect of wave frequency, saturating pore-fluid, volume fraction of fractures and inhomogeneity parameter on the phase velocity and attenuation.
The phenomenon of reflection is studied to calculate the partition of wave-induced energy incident at the plane boundary of the fractured porous solid. The effect of wave frequency, volume fraction of fractures, saturating pore-fluid and inhomogeneity parameter on the energy partition are studied in the numerical example.

Keywords

fractured porous solid, immiscible fluids, propagation, attenuation, reflection coefficients

M. Kumar[a, *] **M. Kumari**[b]

[a]Dept. of Mathematics, Govt. National College Sirsa, India-125 055

[b]Dept. of Mathematics, M. P. College for Women Mandi Dabwali, India-125 104

[*]Author e-mail: *manjit.msc@gmail.com*

1 INTRODUCTION

Fractures play a significant role in hydrology and in many oil and gas reservoirs. In recent years, fractured reservoirs attracted more attention in the research of exploration and production geophysics. The direct prediction of fracture is difficult due to the complexity of the fracture development system. Generally, seismic wave propagation through the Earth (or reservoir rocks)

is strongly affected by the presence of fractures and micro-pores. The type and state of the fluid (liquid or gas) can make a large difference in the response of seismic waves, when these fractures are filled with fluids (oil, gas, water, CO_2, etc.). The studies of elastic wave propagation and related phenomena in fractured porous medium are of great interest in various fields, namely hydrology, nuclear waste industry, petroleum engineering, mining engineering, seismology and exploration of subsurface resources.

The dynamical equations formulated by Biot (1956, 1962a, b) are, generally, used to derive mathematical models for wave propagation studies in poroelastic media. Biot established the fundamental theory for wave propagation in fluid-saturated porous media. It is still well-accepted and forms the basis for wave propagation studies in porous media. This theory successfully predicted the existence of the second compressional wave (the slow compressional wave), which had been observed in the laboratory (Plona 1980; Berryman 1980). Deresiewicz & Skalak (1963) applied the Neumann's uniqueness theorem to poroelasticity and derived the boundary conditions, further which are used to define the boundary value problems for particle dynamics in saturated porous materials.

In general, fractured reservoirs are more complex due to the presence of fractures and pores. Generally, we consider reservoirs containing fractures that are embedded in a porous background. Several treatments of the porous media with fractures have been developed in recent years, which are much closer to real fractured rocks. In addition to matrix porosity and permeability, fracture porosity and fracture permeability also need to be included. As available in the literature, the early models were based on the single porosity or continuum concept. In this approach, a fractured porous medium was grossly treated as an equivalent continuum with a single fluid constituent. A major departure from the single porosity approach was first made by Barenblatt et al. (1960) and Warren & Root (1963). They proposed a phenomenological double porosity model to investigate fluid transport in hydrocarbon reservoirs. They modelled flow through rigid fractured porous media as a complex of two interacting flow regions: one representing the fracture network and the other the porous blocks. The fracture network was characterized by high permeability and low storage, and the porous blocks were characterized by low permeability and high storage. The two flow regions were in turn coupled through a leakage term controlling the transfer of fluid mass between the pores and fractures. An extension of Barenblatt's model to deformable fractured porous media was later given by Duguid & Lee (1977). Aifantis (1977, 1979, 1980) used the theory of mixtures and proposed a coupled double-porosity model for deformable fractured porous media. Alternatives to Aifantis' formulation were given by Wilson and Aifantis (1982), Khaled et al. (1984), Valliappan & Khalili- Naghadeh (1990), Khalili-Naghadeh & Valliappan (1991), Auriault & Boutin (1993) and Bai et al. (1993), among others. Aifantis and his co-workers (Wilson & Aifantis 1982; Beskos & Aifantis 1986; Khaled et al. 1984) published interesting and important series of papers on saturated fractured porous media. It is noted that the final set of governing equations is a direct generalization of Biot's consolidation theory. Wilson & Aifantis (1984) studied the propagation of waves in a saturated fractured porous medium and showed the existence of an extra compressional wave (which appears due to the presence of fractures in the medium), in addition to those encountered in Biot's theory. However, Aifantis model was incomplete, in the sense that it related pore and fracture volume changes only

to the overall volume change of the fractured porous medium. More specifically, it ignored the cross-coupling effects between the volume change of the pores and fractures within the system. This deficiency was eliminated in the formulations proposed by Khalili & Valliappan (1996), Tuncay & Corapcioglu (1996), Wang & Berryman (1996), Khalili et al. (1999), and Loret & Rizzi (1999). Khalili (2003) highlighted the significance of the cross-coupling effects on the pore and fracture fluid pressure response of double-porosity media. Then the credit for comprehensive discussion on wave propagation in fractured porous media saturated with two immiscible viscous fluids goes to Tuncay & Corapcioglu (1996a, b). They derived a general set of coupled partial differential equations to describe the wave propagation through an fractured porous medium permitted by two immiscible viscous fluids. In the absence of volume fractions of the fractures, the constitutive relations reduce to those obtained by Tuncay & Corapciaglu (1997) in the theory of porous media without fractures. Tuncay & Corapcioglu (1996b) studied the propagation of body waves in a fractured porous medium containing two immiscible fluids. They showed that there may exists four compressional waves and one rotational wave. Berryman & Wang (2000) extended Biot's theory of poroelasticity to incorporate the concept of fractures or cracks in the medium, in addition to the generalization to double porosity modelling done in their previous work (Berryman & Wang 1995).

Recently, Arora & Tomer (2010) have considered the reflection and refraction of plane harmonic waves at the boundaries of fractured porous media saturated by two immiscible fluids. In this study, pore-fluids were assumed non-viscous so as to avoid the involvement of attenuation. For the same reason, the incidence was restricted to pre-critical angles. Unfortunately, this is in contrast to the realistic flow mechanics in crustal rocks where the equilibration of fluid pressure produces a great deal of seismic attenuation (Sams et al., 1997). Moreover, the displacements of constituent particles in fractured porous aggregate were subjected to an unintended restriction, which implies that dilatational contribution to the displacement in different constituents comes from different but only one of the four longitudinal waves. However, Sharma & Kumar (2011) and Kumar & Saini (2012) ignored all these restrictions. Sharma & Saini (2012) studied the wave propagation in porous solid containing liquid filled bound pores and two-phase fluid in connected pores. Kumar & Sharma (2013) studied the reflection and transmission of attenuated waves at the boundary between two dissimilar poroelastic solids saturated with two immiscible viscous fluids.

This study considers the propagation of attenuated waves in fractured porous solids saturated with two immiscible viscous fluids. The equation of motion from Tuncay & Corapcioglu (1996a) are solved for propagation of harmonic plane waves. The solution is obtained in the form of Christoffel equations, which provide the complex velocities and polarisations of four attenuated waves in the medium. A particular specification of complex slowness vector is considered to define a general inhomogeneous propagation of attenuated waves. Reflection is studied for the incidence of an inhomogeneous wave at the free plane boundary of the fractured porous medium. An energy matrix is calculated, which defines the shares of five reflected waves in the incident energy. This matrix also identifies the energy due to the interaction between various inhomogeneous waves in the medium. This is required to ensure the conservation of incident energy at the boundary. The effect of wave frequency, volume fraction of fractures, saturating pore-fluid and inhomogeneity

parameter on the energy partition are studied in the numerical example. For convenience, the two immiscible pore-fluids are identified as gas and liquid.

2 FRACTURED POROUS SOLID

2.1 Fundamental equations

In the theory of Tuncay & Corapcioglu (1996a), the presence of fractures in the porous medium is assumed to have two part one can be identified as fractured and other can be non-fractured part. The pores in the non-fractured (fractured) part of the porous medium are referred as primary (secondary) pores. The secondary pores are assumed to be saturated by the wetting fluid, whereas the primary pores are assumed to be saturated by the wetting and non-wetting fluids. Therefore, there are four phases in the system i.e. solid phase, wetting fluid phase in secondary pores, wetting and non-wetting fluid phases in the primary pores. Following Tuncay & Corapcioglu (1996a), under the assumption of no mass exchange between the porous blocks and fractures, the equations of motion for the low-frequency vibrations of constituent particles in isotropic fractured porous solid, in the absence of body forces, are given by

$$\begin{aligned}
\langle\tau_0\rangle_{ij,j} &= \langle\rho_0\rangle\ddot{s}_i - d_1(\dot{u}_i - \dot{s}_i) - d_2(\dot{v}_i - \dot{s}_i) - d_f(\dot{w}_i - \dot{s}_i),\\
\langle\tau_1\rangle_{ij,j} &= \langle\rho_1\rangle\ddot{u}_i + d_1(\dot{u}_i - \dot{s}_i),\\
\langle\tau_2\rangle_{ij,j} &= \langle\rho_2\rangle\ddot{v}_i + d_2(\dot{v}_i - \dot{s}_i),\\
\langle\tau_f\rangle_{ij,j} &= \langle\rho_f\rangle\ddot{w}_i + d_f(\dot{w}_i - \dot{s}_i),
\end{aligned} \tag{1}$$

where the subscripts 0, 1, 2, and f identify the four phases of the fractured porous solid, i.e. solid phase, non-wetting phase, wetting phase in the primary pores, and wetting fluid phase in the fractures, respectively. The τ's are used to define stresses and ρ's are partial densities. The s_i , u_i , v_i and w_i denote the components of displacements of solid, non-wetting fluid, wetting fluid particles in the primary pores, and wetting fluid particles in the fractures, respectively. The indices can take values 1, 2 and 3. A repeated index implies summation. Dot over a variable implies partial derivative with time and comma before an index implies partial space differentiation. Darcy's law relates viscous dissipation to the motion of wetting particles in the secondary pores, wetting and non-wetting fluid particles in the primary pores relative to the pore-walls. The dissipation coefficients for wetting fluid (d_1), non-wetting fluid (d_2), in primary pores and wetting fluid (d_f) in secondary pores are defined as follows.

$$\begin{aligned}
d_1 &= \alpha_p^2\sigma^2\mu_1/(\chi_1 K_p),\\
d_2 &= \alpha_p^2(1-\sigma)^2\mu_2/(\chi_2 K_p),\\
d_f &= \frac{\alpha_p^2\mu_2}{(K_f)},
\end{aligned} \tag{2}$$

where μ_k and χ_k define the viscosity and the relative permeability of fluid phase k. $K_f(K_p)$ denotes the intrinsic permeability of the fractures (non-fractured porous medium). The constitutive relations for four phases system are defined as follows.

$$\begin{aligned}
\langle\tau_0\rangle_{ij} &= \left(a_{11}^{*}s_{k,k} + a_{12}u_{k,k} + a_{13}v_{k,k} + a_{14}w_{k,k}\right)\delta_{ij} + G_{fr}\left(s_{i,j} + s_{j,i}\right),\\
\langle\tau_1\rangle_{ij} &= \left(a_{21}s_{k,k} + a_{22}u_{k,k} + a_{23}v_{k,k} + a_{24}w_{k,k}\right)\delta_{ij},\\
\langle\tau_2\rangle_{ij} &= \left(a_{31}s_{k,k} + a_{32}u_{k,k} + a_{33}v_{k,k} + a_{34}w_{k,k}\right)\delta_{ij},\\
\langle\tau_f\rangle_{ij} &= \left(a_{41}s_{k,k} + a_{42}u_{k,k} + a_{43}v_{k,k} + a_{44}w_{k,k}\right)\delta_{ij},
\end{aligned} \tag{3}$$

where δ_{ij} is Kronecker symbol. G_{fr} is the shear modulus of solid matrix. The elastic constants used in the above equations are given in Appendix.

In terms of the displacement components, the equations of motion are expressed as follows.

$$\begin{aligned}
a_{11}^{**}s_{j,ij} + a_{12}u_{j,ij} + a_{13}v_{j,ij} + a_{14}w_{j,ij} + G_{fr}s_{i,jj} + d_1(\dot{u}_i - \dot{s}_i)\\
+d_2(\dot{v}_i - \dot{s}_i) + d_f(\dot{w}_i - \dot{s}_i) = \langle\rho_0\rangle\ddot{s}_i,\\
a_{21}s_{j,ij} + a_{22}u_{j,ij} + a_{23}v_{j,ij} + a_{24}w_{j,ij} - d_1(\dot{u}_i - \dot{s}_i) = \langle\rho_1\rangle\ddot{u}_i,\\
a_{31}s_{j,ij} + a_{32}u_{j,ij} + a_{33}v_{j,ij} + a_{34}w_{j,ij} - d_2(\dot{v}_i - \dot{s}_i) = \langle\rho_2\rangle\ddot{v}_i,\\
a_{41}s_{j,ij} + a_{42}u_{j,ij} + a_{43}v_{j,ij} + a_{44}w_{j,ij} - d_f(\dot{w}_i - \dot{s}_i) = \langle\rho_f\rangle\ddot{w}_i.
\end{aligned} \tag{4}$$

2.2 Plane wave propagation

To seek the harmonic solution of system of equations (4), for the propagation of plane waves, the displacement components are written as follows.

$$\left(s_j, u_j, v_j, w_j\right) = \left(S_j, G_j, L_j, K_j\right)exp\{\iota\omega(p_k x_k - t)\}, \qquad (j = 1,2,3) \tag{5}$$

where ω is angular frequency and (p_1, p_2, p_3) is slowness vector $\mathbf{p}$. The vectors $\boldsymbol{S} = (S_1, S_2, S_3)^T, \boldsymbol{G} = (G_1, G_2, G_3)^T$ and $\boldsymbol{L} = (L_1, L_2, L_3)^T$, and $\boldsymbol{K} = (K_1, K_2, K_3)^T$ define, respectively, the polarizations for the motions of the solid, non-wetting fluid and wetting fluid particles in primary pores, and wetting fluid particles in secondary pores in the composite medium. Substituting (5) in (4) yields a system of twelve equations, given by

$$\begin{aligned}
\left[a_{11}^{**}\mathbf{p}^{\mathrm{T}}\mathbf{p} - \left\{<\rho_0> + \frac{\iota}{\omega}(d_1 + d_2 + d_f) - G_{fr}\mathbf{p}\mathbf{p}^{\mathrm{T}}\right\}\mathbf{I}\right]\mathbf{S} + \left(a_{12}\mathbf{p}^{\mathrm{T}}\mathbf{p} + \frac{\iota}{\omega}d_1\mathbf{I}\right)\mathbf{G}\\
+\left(a_{13}\mathbf{p}^{\mathrm{T}}\mathbf{p} + \frac{\iota}{\omega}d_2\mathbf{I}\right)\mathbf{L} + \left(a_{14}\mathbf{p}^{\mathrm{T}}\mathbf{p} + \frac{\iota}{\omega}d_f\mathbf{I}\right)\mathbf{K} = 0,
\end{aligned} \tag{6}$$

$$\left(a_{21}\mathbf{p}^{\mathrm{T}}\mathbf{p} + \frac{\iota}{\omega}d_1\mathbf{I}\right)\mathbf{S} + (a_{22}\mathbf{p}^{\mathrm{T}}\mathbf{p} - \rho_1\mathbf{I})\mathbf{G} + a_{23}\mathbf{p}^{\mathrm{T}}\mathbf{p}\mathbf{L} + a_{24}\mathbf{p}^{\mathrm{T}}\mathbf{p}\mathbf{K} = 0, \quad \rho_1 = <\rho_1> + \frac{\iota}{\omega}d_1, \tag{7}$$

$$\left(a_{31}\mathbf{p}^{\mathrm{T}}\mathbf{p} + \frac{\iota}{\omega}d_2\mathbf{I}\right)\mathbf{S} + a_{32}\mathbf{p}^{\mathrm{T}}\mathbf{p}\mathbf{G} + (a_{33}\mathbf{p}^{\mathrm{T}}\mathbf{p} - \rho_2\mathbf{I})\mathrm{L} + a_{34}\mathbf{p}^{\mathrm{T}}\mathbf{p}\mathbf{K} = 0, \quad \rho_2 = <\rho_2> + \frac{\iota}{\omega}d_2, \tag{8}$$

$$\left(a_{41}\mathbf{p}^{\mathrm{T}}\mathbf{p} + \frac{\iota}{\omega}d_f\mathbf{I}\right)\mathbf{S} + a_{42}\mathbf{p}^{\mathrm{T}}\mathbf{p}\mathbf{G} + a_{43}\mathbf{p}^{\mathrm{T}}\mathbf{p}\mathbf{L} + (a_{44}\mathbf{p}^{\mathrm{T}}\mathbf{p} - \rho_f\mathbf{I})\mathbf{K} = 0, \quad \rho_f = <\rho_f> + \frac{\iota}{\omega}d_f, \tag{9}$$

where $\mathbf{p}^T$ denotes the transpose of $\mathbf{p}$. The equations (7), (8) and (9) of this system are solved into three relations, given by

$$\mathbf{G} = \mathbf{AS}, \qquad \mathbf{A} = \frac{\iota}{\omega}\frac{\mathrm{d}_1}{\rho_1}\mathbf{I} + \frac{\mathrm{Z}_{11}\Lambda + \mathrm{Z}_{10}}{\mathrm{a}'\Lambda^2 + \mathrm{b}'\Lambda + \mathrm{c}'}\mathbf{p}^{\mathrm{T}}\mathbf{p}, \qquad \Lambda = \mathbf{p}\mathbf{p}^{\mathrm{T}}, \tag{10}$$

$$\mathbf{L} = \mathbf{BS}, \qquad \mathbf{B} = \frac{\iota}{\omega}\frac{\mathrm{d}_2}{\rho_2}\mathbf{I} + \frac{\mathrm{Z}_{21}\Lambda+\mathrm{Z}_{20}}{\mathrm{a}'\Lambda^2+\mathrm{b}'\Lambda+\mathrm{c}'}\mathbf{p}^{\mathrm{T}}\mathbf{p}, \tag{11}$$

$$\mathbf{K} = \mathbf{CS}, \qquad \mathbf{C} = \frac{\iota}{\omega}\frac{\mathrm{d}_\mathrm{f}}{\rho_\mathrm{f}}\mathbf{I} - \frac{\mathrm{Z}_{32}\Lambda^2 + \mathrm{Z}_{31}\Lambda + \mathrm{Z}_{30}}{(\mathrm{a}_{44}\Lambda - \rho_\mathrm{f})(\mathrm{a}'\Lambda^2 + \mathrm{b}'\Lambda + \mathrm{c}')}\mathbf{p}^{\mathrm{T}}\mathbf{p}, \tag{12}$$

which relate the polarisations (or displacements) of particles of solid, non-wetting and wetting fluid phases in the primary pores, and wetting fluid in secondary pores in the composite medium. Using these relations in (6) yields a system of three equations, given by

$$\Gamma\mathbf{S} = \mathbf{0}, \qquad \Gamma = \gamma_1\mathbf{p}^{\mathrm{T}}\mathbf{p} + \gamma_2(\Lambda\mathbf{I} - \mathbf{p}^{\mathrm{T}}\mathbf{p}), \tag{13}$$

which are the Christoffel equations for the propagation of harmonic plane waves in the fractured porous medium saturated by two immiscible fluids. The coefficients used in various relations are defined as follows.

$$\gamma_1 = \left(G_{fr} + d'\right)\Lambda + \frac{\Gamma_{13}\Lambda^3 + \Gamma_{12}\Lambda^2 + \Gamma_{11}\Lambda + \Gamma_{10}}{r_3\Lambda^3 + r_2\Lambda^2 + r_1\Lambda + r_0}\Lambda - \rho_s, \qquad \gamma_2 = G_{fr}\Lambda - \rho_s,$$

$$\rho_s = <\rho_0> + \frac{\iota}{\omega}\mathrm{d}_1\left(1 - \frac{\iota}{\omega}\frac{\mathrm{d}_1}{\rho_1}\right) + \frac{\iota}{\omega}\mathrm{d}_2\left(1 - \frac{\iota}{\omega}\frac{\mathrm{d}_2}{\rho_2}\right) + \frac{\iota}{\omega}\mathrm{d}_\mathrm{f}\left(1 - \frac{\iota}{\omega}\frac{\mathrm{d}_\mathrm{f}}{\rho_\mathrm{f}}\right),$$

$$a' = a_{22}a_{33} - a_{23}a_{32}, \qquad b' = -(a_{22}\rho_2 + a_{33}\rho_1), \qquad c' = \rho_1\rho_2,$$

$$d' = a_{11}^{**} + \frac{\iota}{\omega}\left(a_{12}\frac{d_1}{\rho_1} + a_{13}\frac{d_2}{\rho_2} + a_{14}\frac{d_f}{\rho_f}\right),$$

$$r_3 = a'a_{44}, \quad r_2 = b'a_{44} - a'\rho_f, \quad r_1 = \rho_1\rho_2a_{44} - b'\rho_f, \qquad r_0 = -\rho_1\rho_2\rho_f,$$

$$\Gamma_{13} = a_{44}(a_{12}Z_{11} + a_{13}Z_{21}) - a_{14}Z_{32},$$

$$\Gamma_{12} = a_{44}\left\{a_{12}Z_{10} + a_{13}Z_{20} + \frac{\iota}{\omega}(d_1Z_{11} + d_2Z_{21})\right\} - \rho_f(a_{12}Z_{11} + a_{13}Z_{21}) - a_{14}Z_{31} - \frac{\iota}{\omega}d_fZ_{32},$$

$$\Gamma_{11} = \frac{i}{\omega} a_{44}(d_1 Z_{10} + d_2 Z_{20}) - \rho_f \left\{ \frac{\iota}{\omega} (d_1 Z_{11} + d_2 Z_{21}) + a_{12} Z_{10} + a_{13} Z_{20} \right\} - a_{14} Z_{30} - \frac{\iota}{\omega} d_f Z_{31},$$

$$\Gamma_{10} = -\rho_f \frac{\iota}{\omega} (d_1 Z_{10} + d_2 Z_{20}) - \rho_f \frac{\iota}{\omega} Z_{30},$$

$$Z_{11} = a_1 - \frac{\iota}{\omega} \frac{d_1}{\rho_1} a', \qquad Z_{10} = b_1 - \frac{\iota}{\omega} \frac{d_1}{\rho_1} b',$$

$$Z_{21} = a_2 - \frac{\iota}{\omega} \frac{d_2}{\rho_2} a', \qquad Z_{20} = b_2 - \frac{\iota}{\omega} \frac{d_2}{\rho_2} b',$$

$$Z_{32} = a_1 a_{42} + a_2 a_{43} + a' \left(a_{41} + \frac{\iota}{\omega} \frac{d_f}{\rho_f} a_{44} \right),$$

$$Z_{31} = b_1 a_{42} + b_2 a_{43} + b' \left(a_{41} + \frac{\iota}{\omega} \frac{d_f}{\rho_f} a_{44} \right),$$

$$Z_{30} = \rho_1 \rho_2 \left(a_{41} + \frac{\iota}{\omega} \frac{d_f}{\rho_f} a_{44} \right) + \frac{\iota}{\omega} (d_1 \rho_2 a_{42} + d_2 \rho_1 a_{43}),$$

$$a_1 = (a_{23} a_{31} - a_{21} a_{33}) + \frac{\iota}{\omega} \frac{d_f}{\rho_f} (a_{23} a_{34} - a_{24} a_{33}),$$

$$a_2 = (a_{21} a_{32} - a_{22} a_{31}) + \frac{\iota}{\omega} \frac{d_f}{\rho_f} (a_{24} a_{32} - a_{22} a_{34}),$$

$$b_1 = \rho_2 \left(a_{21} + a_{24} \frac{\iota}{\omega} \frac{d_f}{\rho_f} \right) + \frac{\iota}{\omega} (d_2 a_{23} - d_1 a_{33}),$$

$$b_2 = \rho_1 \left(a_{31} + a_{34} \frac{\iota}{\omega} \frac{d_f}{\rho_f} \right) + \frac{\iota}{\omega} (d_1 a_{32} - d_2 a_{22}).$$

2.3 Five attenuated waves

In terms of velocity V, the slowness is defined as $\mathbf{p} = \mathbf{N}/\mathrm{V}$ such that $\mathbf{N}\mathbf{N}^{\mathrm{T}} = 1$ and $\Lambda = 1/\mathrm{V}^2$. The dual (complex) vector $\mathbf{N}$ represents the directions of propagation and attenuation of a wave in the fractured porous medium. In terms of $\mathbf{N}$ and V, the Christoffel equations (13) are expressed as

$$[\gamma_1 \mathbf{N}^{\mathrm{T}} \mathbf{N} + \gamma_2 (\mathbf{I} - \mathbf{N}^{\mathrm{T}} \mathbf{N})] \mathbf{S} = 0. \tag{14}$$

The non-trivial solution for Christoffel equations is ensured by vanishing the determinant $(=\gamma_1\gamma_2^2)$ of the matrix $\gamma_1\mathbf{N}^{\mathrm{T}}\mathbf{N}+\gamma_2(\mathbf{I}-\mathbf{N}^{\mathrm{T}}\mathbf{N})$. This condition translates into two equations as follows.

The first one (i.e. $\gamma_1=0$) implies that

$$\begin{aligned} r_0\rho_s\lambda^4+[r_1\rho_s-r_0(G_{fr}+d')-\Gamma_{10}]\lambda^3+[r_2\rho_s-r_1(G_{fr}+d')-\Gamma_{11}]\lambda^2 \\ +[r_3\rho_s-r_2(G_{fr}+d')-\Gamma_{12}]\lambda-[r_3(G_{fr}+d')+\Gamma_{13}]=0,\ \ \lambda=V^2. \end{aligned} \tag{15}$$

Four roots of this complex biquadratic equation define the complex velocities $(V_j,\ j=1,2,3,4)$ of four attenuating waves in the dissipative porous medium. In this case the polarization tor (S_1,S_2,S_3), corresponding to equation (14), is calculated to be parallel to $\mathbf{N}$ and hence the four waves identified with velocities V_1,V_2,V_3 and V_4 are longitudinal waves.

Another equation (i.e. $\gamma_2=0$) yields

$$\rho_sV^2-G_{fr}=0, \tag{16}$$

which implies a wave with complex velocity $V_5=\sqrt{G_{fr}/\rho_s}$. The corresponding polarization vector (S_1,S_2,S_3), is represented through a singular matrix $(\mathbf{I}-\mathbf{N}^{\mathrm{T}}\mathbf{N})$. So, the polarization vector may be parallel to a column (or, row) vector of this symmetric matrix. This defines the direction of polarisation in a plane, which is normal to the propagation vector $\mathbf{N}$. This implies that the attenuated wave with velocity V_5 is a transverse wave.

The polarisation vector $\mathbf{S}$ defines the polarisation of solid particles in the fractured porous medium. Polarisations of the non-wetting, wetting fluid particles in primary pores and wetting fluid particles in secondary pores are calculated from the relations (10), (11) and (12), respectively. For convenience in discussion, the four longitudinal waves with velocity order $\Re(V_1)>R(V_2)>R(V_3)>R(V_4)$ are named as P_1,P_2,P_3,P_4 waves, respectively. The lone transverse wave is identified as S wave.

3 INHOMOGENEOUS PLANE WAVES

The general plane waves propagating in a dissipative medium are inhomogeneous waves (Borcherdt 1982). The propagation of an attenuated wave is defined with complex slowness vector. The real and imaginary parts of complex slowness vector are termed as propagation vector and attenuation vector, respectively. In general, the inhomogeneity of an attenuating wave is represented through the difference in the directions of its propagation vector and attenuation vector. In other words, an angle between equi-amplitude plane and equi-phase plane of an attenuating plane wave represent its inhomogeneous character. However, some restrictions may be needed on the choice of this inhomogeneity angle. The invalid values of the inhomogeneity angle are termed as forbidden directions, which were discovered first in the pioneering works of Krebes & Le (1994) and Carcione & Cavallini (1995). As an alternative to this conventional representation, Sharma (2008) used a finite non-dimensional parameter to define inhomogeneous waves in anisotropic

media. In terms of this inhomogeneity parameter (δ), the complex slowness vector $\mathbf{p}$ of an attenuated wave is written as follows.

$$\mathbf{p} = \frac{1}{\mathrm{c}}[\hat{\mathbf{n}} + \iota\beta\hat{\mathbf{n}} + \iota\delta\hat{\mathbf{m}}], \tag{17}$$

where the propagation direction $\hat{\mathbf{n}}$ and an orthogonal unit vector $\hat{\mathbf{m}}$ identifies the propagation-attenuation plane. The total attenuation is a vector sum of two orthogonal vectors. The first one, $(\beta/c)\hat{\mathbf{n}}$, defines the attenuation along the direction of propagation. Hence, it represents the homogeneous wave and its contribution β/c to total attenuation is termed as homogeneous attenuation. The other part $(\delta/c)\hat{\mathbf{m}}$ in (17) then represents the contribution of inhomogeneous propagation of wave to total attenuation $\left(\sqrt{(\beta^2+\delta^2)}/c\right)$. For $\delta = 0$, the attenuated wave is considered to be propagating as homogeneous wave. This implies that inhomogeneous propagation of the attenuated wave is represented through the deviation of δ from zero. Hence, the magnitude of inhomogeneity parameter δ is considered as the strength of the inhomogeneous wave. For known values of propagation direction $\hat{\mathbf{n}}$, orthogonal direction $\hat{\mathbf{m}}$ and inhomogeneity parameter $\delta \in [0,1)$, we need to determine the attenuation coefficient β and the phase velocity c . It may be noted that the sign of δ does not affect the values of β and c. Using the relations $\mathbf{p}$=$\mathbf{N}$/V and $\mathbf{N}\mathbf{N}^{\mathrm{T}} = 1$ in (17), we get

$$c^2 = -2\beta\frac{|\lambda|^2}{\Im(\lambda)}, \quad \beta = \frac{\Re(\lambda)}{\Im(\lambda)} + \sqrt{\left(\frac{\Re(\lambda)}{\Im(\lambda)}\right)^2 + 1 - \delta^2}, \quad \mathbf{N} = \frac{(1+\iota\beta)\hat{\mathbf{n}} + \iota\delta\hat{\mathbf{m}}}{\sqrt{1-\beta^2-\delta^2+\iota 2\beta}}. \tag{18}$$

The quality factor of attenuation (i.e. Q) for a wave is defined as

$$Q^{-1} = -\frac{\Im(\lambda)}{\Re(\lambda)} = \frac{2\beta}{1-\beta^2-\delta^2}. \tag{19}$$

The equations (15) and (16) do not involve $\mathbf{N}$. That means, for a chosen medium, the value of $\lambda(=V^2)$ is independent of $\mathbf{N}$. It may be noted that a change in δ can affect λ only through $\mathbf{N}$. This implies that for any value of δ (in other words, $\mathbf{N}$), the λ will be same. Then, from the first equality in (19), this implies a constant Q^{-1} for each attenuated wave in the medium. Then the effect of wave inhomogeneity (i.e. δ) on attenuation may be observed in an attenuation coefficient given by

$$\zeta = \frac{\omega\sqrt{\beta^2+\delta^2}}{c}. \tag{20}$$

For the homogeneous propagation (i.e. $\delta = 0$) of an attenuated wave, the above defined relations reduce to

$$c = \frac{|V|^2}{\Re(V)}, \quad \beta = -\frac{\Im(V)}{\Re(V)}, \quad \mathbf{N} = \hat{\mathbf{n}}, \qquad \zeta = \omega\frac{\beta}{c}. \tag{21}$$

The other extreme value of δ (=1) implies $\beta = 0$ and then slowness vector $\mathbf{p} = (\hat{\mathbf{n}} + \iota\hat{\mathbf{m}})/c$ defines a wave with attenuation direction orthogonal to its propagation direction, i.e. evanescent wave.

4 REFLECTION AT PLANE BOUNDARY

The present study aims to analyse the propagation and attenuation of five reflected waves arising from the incidence of an inhomogeneous wave at the free plane surface of a fractured porous solid saturated with two immiscible fluids (non-wetting and wetting).

4.1 Definition of the problem

Consider a rectangular coordinate system (x_1, x_2, x_3) to represent a three-dimensional space. The half-space $x_3 \geq 0$ is occupied by a saturated fractured porous solid with its depth increasing along the x_3-direction. The plane $x_3 = 0$ is the surface of this medium. The medium being isotropic, the propagation and attenuation of waves are considered in a plane and this plane is assumed to be a coordinate (i.e. $x_1 - x_3$) plane. In this plane, a wave travels towards the surface and become incident at a point on the surface making an angle θ with the x_3-axis. Then the propagation direction $\hat{\mathbf{n}} = (\sin\theta, 0, -\cos\theta)$ and its orthogonal direction $\hat{\mathbf{m}} = (\cos\theta, 0, \sin\theta)$ identify the $x_1 - x_3$ plane as the propagation-attenuation plane. The incident wave can be any of the five attenuated waves in the fractured porous medium. For an arbitrarily chosen value of inhomogeneity parameter $\delta \in [0,1)$, the values of β and c for this incident wave are calculated from (18). Using all these values, the slowness vector is calculated for the incident wave as $(p_1, 0, q_0)$ such that $q_0 = \sqrt{\frac{1}{V_0^2} - p_1^2}$, where V_0 denotes the complex velocity of the incident wave. Being a square-root of a complex quantity, the value for q_0 is chosen such that $\Re(q_0) < 0$. In the present geometry of the medium, this restriction ensures the propagation of incident wave towards the surface $x_3 = 0$. The incident wave results in five waves (P_1, P_2, P_3, P_4, S) reflected back into the porous medium. Snell's law implies that horizontal slowness of each of the reflected wave will be same as that of incident wave, i.e. p_1. Then the slowness vectors for the reflected waves are written as $(p_1, 0, q_k)$, $q_k = \sqrt{\frac{1}{V_k^2} - p_1^2}$, $(k = 1,2,3,4,5)$. The decay of a reflected wave along positive x_3-direction is ensured with the positive value for imaginary part of corresponding q_k.

4.2 Displacements

The displacement of solid particles in the fractured porous medium due to the presence of an incident wave and five reflected waves is expressed as follows.

$$s_j = S_j^{(0)} exp\{\iota\omega(p_1 x_1 + q_0 x_3 - t)\} + \sum_{k=1}^{5} f_k S_j^{(k)} exp\{\iota\omega(p_1 x_1 + q_k x_3 - t)\}, \ \ (j = 1,3), \tag{22}$$

where f_k are the excitation factors for reflected waves relative to incident wave. The complex vector $\left(S_1^{(k)}, 0, S_3^{(k)}\right)$ defines the polarisation and phase shift of the motion of solid particles for incident wave (k=0) and reflected waves (k=1,2,3,4,5). The corresponding displacements of the non-wetting, wetting fluid particles in primary pores and wetting fluid particles in secondary pores can be calculated from the relations (10), (11) and (12) using the wave-specific values of the matrices **A**, **B** and **C**, respectively.

4.3 Boundary conditions

Surface of the fractured porous solid is considered to be free of stresses. Hence, at every point on the surface of material, the resultant energy must vanish. This is achieved through the equation

$$\sum_{j=n,t} \left(< \tau_0 >_{nj} \dot{s}_j\right) + < \tau_1 >_{nn} \dot{u}_n + < \tau_2 >_{nn} \dot{v}_n + < \tau_f >_{nn} \dot{w}_n = 0. \tag{23}$$

The index n (or, t) is used to denote the component normal (or, tangential) to the surface. The repetition of index n in this section does not imply summation. The boundary conditions at the surface
are obtained from the physical conditions there, subjected to the energy constraint defined in (23). So, at the stress-free surface of fractured porous medium, the aggregate stress from the solid phase (i.e., $< \tau_0 >_{nj}$), non-wetting phase $< \tau_1 >_{nn}$, wetting phase $< \tau_2 >_{nn}$ in the primary pores, and $< \tau_f >_{nn}$ wetting fluid phase in secondary pores together should vanish. For sealed surface pores, there will be no fluid discharge (i.e. $\dot{u}_n - \dot{s}_n = \dot{v}_n - \dot{s}_n = \dot{w}_n - \dot{s}_n = 0$) at the surface. Hence, the appropriate boundary conditions to be satisfied at the stress-free surface $x_3 = 0$ are given by

$i) \ < \tau_0 >_{33} + < \tau_1 >_{33} + < \tau_2 >_{33} + < \tau_f >_{33} = 0, \qquad ii) \ < \tau_0 >_{31} = 0,$
$iii) \dot{u}_3 - \dot{s}_3 = 0, \ \ iv) \ \dot{v}_3 - \dot{s}_3 = 0, \ \ v) \ \ \dot{w}_3 - \dot{s}_3 = 0.$

The equations (3) relate the stress components in different phases to the displacements of particles. The above boundary conditions are satisfied through a system of five linear inhomogeneous equations in f_1, f_2, f_3, f_4 and f_5. This system of equations is given by,

$$\sum_{j=1}^{5} b_{ij} f_j = -b_{i0}, \ \ (i = 1,2,3,4,5), \tag{24}$$

where the coefficients b_{ij}, (i=1,2,3,4,5; j=0,1,2,3,4,5), are expressed as follows.

$$b_{1j} = \left(W_{11}^{(j)} + X_{11}^{(j)} + Y_{11}^{(j)} + Z_{11}^{(j)}\right) p_1 S_1^{(j)} + \left(W_{33}^{(j)} + X_{33}^{(j)} + Y_{33}^{(j)} + Z_{33}^{(j)} + 2G_{fr}\right) q_j S_3^{(j)},$$

$$b_{2j} = q_j S_1^{(j)} + p_1 S_3^{(j)},$$
$$b_{3j} = \left[A_{31}^{(j)} S_1^{(j)} + \left(A_{33}^{(j)} - 1\right) S_3^{(j)}\right],$$
$$b_{4j} = \left[B_{31}^{(j)} S_1^{(j)} + \left(B_{33}^{(j)} - 1\right) S_3^{(j)}\right],$$
$$b_{5j} = \left[C_{31}^{(j)} S_1^{(j)} + \left(C_{33}^{(j)} - 1\right) S_3^{(j)}\right].$$

The matrices used in the above expressions are defined as

$$\mathbf{W}^{(j)} = a_{11}^{*}\mathbf{I} + a_{12}\mathbf{A}^{(j)} + a_{13}\mathbf{B}^{(j)} + a_{14}\mathbf{C}^{(j)},$$
$$\mathbf{X}^{(j)} = a_{21}\mathbf{I} + a_{22}\mathbf{A}^{(j)} + a_{23}\mathbf{B}^{(j)} + a_{24}\mathbf{C}^{(j)},$$
$$\mathbf{Y}^{(j)} = a_{31}\mathbf{I} + a_{32}\mathbf{A}^{(j)} + a_{33}\mathbf{B}^{(j)} + a_{34}\mathbf{C}^{(j)},$$
$$\mathbf{Z}^{(j)} = a_{41}\mathbf{I} + a_{42}\mathbf{A}^{(j)} + a_{43}\mathbf{B}^{(j)} + a_{44}\mathbf{C}^{(j)},$$

where the superscript $'(j)'$ on matrices **A, B** and **C** means the matrices are evaluated for slowness vector **p** of the corresponding wave represented with a value of j (=0,1,2,3,4,5).

4.4 Energy ratios

Distribution of incident energy among different reflected waves is considered across a surface element of unit area at the plane $x_3 = 0$. Following Achenbach (1973), the scalar product of surface traction and particle velocity per unit area, denoted by P^*, represents the rate at which the energy is communicated per unit area of the surface. The time average of P^*, over a period, denoted by $< P^* >$, represents the average energy transmission per unit surface area per unit time. For a surface with normal along the x_3-direction, the average energy flux is represented through the components $< P_{ij}^* >$ given by

$$\begin{aligned} < P_{ij}^* > = {} & \Re\left(< \tau_0 >_{31}^{(i)}\right)\Re\left(\dot{s}_1^{(j)}\right) + \Re\left(< \tau_0 >_{33}^{(i)}\right)\Re\left(\dot{s}_3^{(j)}\right) + \Re\left(< \tau_1 >_{33}^{(i)}\right)\Re\left(\dot{u}_3^{(j)}\right) \\ & + \Re\left(< \tau_2 >_{33}^{(i)}\right)\Re\left(\dot{v}_3^{(j)}\right) + \Re\left(< \tau_f >_{33}^{(i)}\right)\Re\left(\dot{w}_3^{(j)}\right). \end{aligned} \tag{25}$$

The incidence of a general inhomogeneous wave involves the concept of interaction energy (Borcherdt 1982; Krebes 1983) or the interference energy (Ainslie & Burns 1995) between the dissimilar pairs of incident and reflected waves in the medium. To explain the distribution of incident energy at the free surface of a dissipative fractured porous medium, a matrix is defined with its elements given by

$$E_{ij} = -\frac{\Re\left(F_{ij} f_i \bar{f}_j\right)}{\Re(F_{00})}, \qquad (i, j = 0,1,2,3,4,5), \tag{26}$$

where bar over an entity implies its complex conjugate. The elements of matrix **F** are defined as follows.

$$F_{ij} = \left[G_{fr} q_i + \left(X_{11}^{(i)} \bar{A}_{31}^{(j)} + Y_{11}^{(i)} \bar{B}_{31}^{(j)} + Z_{11}^{(i)} \bar{C}_{31}^{(j)}\right) p_1\right] S_1^{(i)} \bar{S}_1^{(j)} \tag{27}$$

$$+\left[G_{fr}p_1+\left(X_{33}^{(i)}\bar{A}_{31}^{(j)}+Y_{33}^{(i)}\bar{B}_{31}^{(j)}+Z_{33}^{(i)}\bar{C}_{31}^{(j)}\right)q_i\right]S_3^{(i)}\bar{S}_1^{(j)}$$
$$+\left[W_{11}^{(i)}+X_{11}^{(i)}\bar{A}_{33}^{(j)}+Y_{11}^{(i)}\bar{B}_{33}^{(j)}+Z_{11}^{(i)}\bar{C}_{33}^{(j)}\right]p_1S_1^{(i)}\bar{S}_3^{(j)}$$
$$+\left[2G_{fr}+W_{33}^{(i)}+X_{33}^{(i)}\bar{A}_{33}^{(j)}+Y_{33}^{(i)}\bar{B}_{33}^{(j)}+Z_{33}^{(i)}\bar{C}_{33}^{(j)}\right]q_iS_3^{(i)}\bar{S}_3^{(j)}.$$

Solving the system of equations (24), by Gauss elimination method, provides the values for excitation factors (f_i), which are required to calculate the matrix (26) for $x_3 = 0$. This energy matrix explains the energy partition at the boundary $x_3 = 0$ of the porous solid. The sum of all the non-diagonal entries of this energy matrix calculates the share of interaction energy in the medium. The diagonal entries $E_{11}, E_{22}, E_{33}, E_{44}$ and E_{55} of this matrix denote the energy shares of reflected (P_1, P_2, P_3, P_4) and S waves in the incident energy. The energy due to the interaction of incident wave with the five reflected waves is given by $E_{IR} = \sum_{i=1}^{5}\left(\sum_{j=1}^{5} E_{ij} - E_{ii}\right)$. The energy due to the interaction among the five reflected waves is given by $E_{RR} = \sum_{i=1}^{5}\left(\sum_{j=1}^{5} E_{ij} - E_{ii}\right)$. Then the conservation of energy at the free-surface is ensured through the relation

$$E_{11} + E_{22} + E_{33} + E_{44} + E_{55} + E_{IR} + E_{RR} = -E_{00} = 1. \tag{28}$$

5 NUMERICAL RESULTS AND DISCUSSION

5.1 Numerical example

In order to investigate the dependence of velocities, amplitude ratios and energy ratios on the various material parameters, a numerical study was conducted in MATLAB for an illustrative example. A fractured sandstone (rock) saturated with air and water is chosen for the numerical model of fractured porous medium (Tuncay & Corapcioglu 1996). The solid grains of the rock with bulk modulus $K_s = 35.00GPa$, shear modulus $G_{fr} = 1.02GPa$, and density $\rho_0 = 2650Kg/m^3$ form a porous frame of porosity $\phi = 0.25$. The primary pore space (i.e., non-fractured part) is filled with the gas of bulk modulus $K_1' = 0.145MPa$, density $\rho_1 = 1.1Kg/m^3$, relativity permeability $\chi_1 = 0.88$ and viscosity $\mu_1 = 1.8 \times 10^{-6} Pa.s$ mixed in water of bulk modulus $K_2' = 2.25GPa$, $\rho_2 = 997Kg/m^3$, relativity permeability $\chi_2 = 0.001$ and viscosity $\mu_2 = 10^{-3} Pa.s$. The secondary pore space (i.e., fractured part) is filled with the water having same density and viscosity as water in primary pore. The bulk modulus $K_{fr} = 1.44GPa$ and $K_{fr}^m = 3.00GPa$ of fractured and non-fractured medium, respectively. Intrinsic permeability $K_f = 10^{-11}m^2$ and $K_p = 10^{-13}m^2$ of fractured and non-fractured medium, respectively. A dimensionless material parameter $F = 0.8$. The value of $P_{cap}' = 0.1MPa$ is used to represent capillary pressure. The secondary pore space (i.e., fractured part) is filled with the water having same density and viscosity as water in primary pore. For computation purposes, Low-frequency propagation is ensured with $\omega \leq 2\pi \times 5kHz$.

5.2 Velocity and attenuation

The numerical values of various parameters given above are used to calculate the complex velocities of the five attenuated (i.e. P_1, P_2, P_3, P_4, S) waves in the fractured porous medium. Phase velocities $(c_j, j = 1,2,3,4,5)$ and attenuation coefficients $(\zeta_j, j = 1,2,3,4,5)$ are computed for inhomoge-

neous propagation of these waves. Effect of various parameters on c_j and ζ_j are exhibited in Fig. 1-Fig. 4

Effect of frequency

The variations of phase velocities and attenuation coefficients of the P_1, P_2, P_3, P_4 and S waves with $\delta \in [0,1)$ are exhibited in Fig. 1 for three different frequencies, $\omega/2\pi = 0.1, 1, 5\text{kHz}$. Values chosen for other parameters are $\alpha_f = 0.01, \sigma = 0.5$. It is quite evident that with the increase of inhomogeneity of an attenuated wave of given frequency, its phase velocity decreases but attenuation increases. The velocity of three (P_1, P_2, S) waves may reduce up to one-half with the change in propagation from homogeneous to evanescent. The increase of frequency may not have much effect on the velocity of (P_1, S) waves. However, the three slower longitudinal (i.e. P_2, P_3, P_4) waves propagate faster at higher frequency. At low-frequency, the velocity of (P_3, P_4) waves may not decrease much with the increase of inhomogeneity strength. For each of the five waves in porous medium, an increase of frequency (and/or inhomogeneity) increases its attenuation. However, the effect of inhomogeneity on attenuation may be mild at low frequencies. The general observations are that slower the propagation higher is the attenuation and homogeneous waves may travel faster but cannot represent the wave motion with larger attenuation.

Effect of gas share in pores

The variations of phase velocities and attenuation coefficients of the five (i.e. P_1, P_2, P_3, P_4, S) waves with $\delta \in [0,1)$ are presented in Fig. 2, for three different values $\sigma = 0.01, 0.5, 0.99$ of gas saturation. Values chosen for other parameters are $\alpha_f = 0.02, \omega/2\pi = 1\text{kHz}$. A smaller gas share in pores means more liquid in pores and vice-verse. The limiting values of σ (i.e., 0, 1) are avoided for representing the non-realistic situations of no gas/all liquid and all gas/no liquid. The increase of gas share increases the velocity of S wave whereas three longitudinal waves (i.e. P_1, P_2, P_3) travel faster when the pore space is filled only with liquid. However, the slowest travel of longitudinal waves may be expected when pore space is equally shared by the two fluids. It is quite evident that the variations of the velocity of a wave with gas share in the pores appear nearly opposite to the variations in its attenuation coefficient.

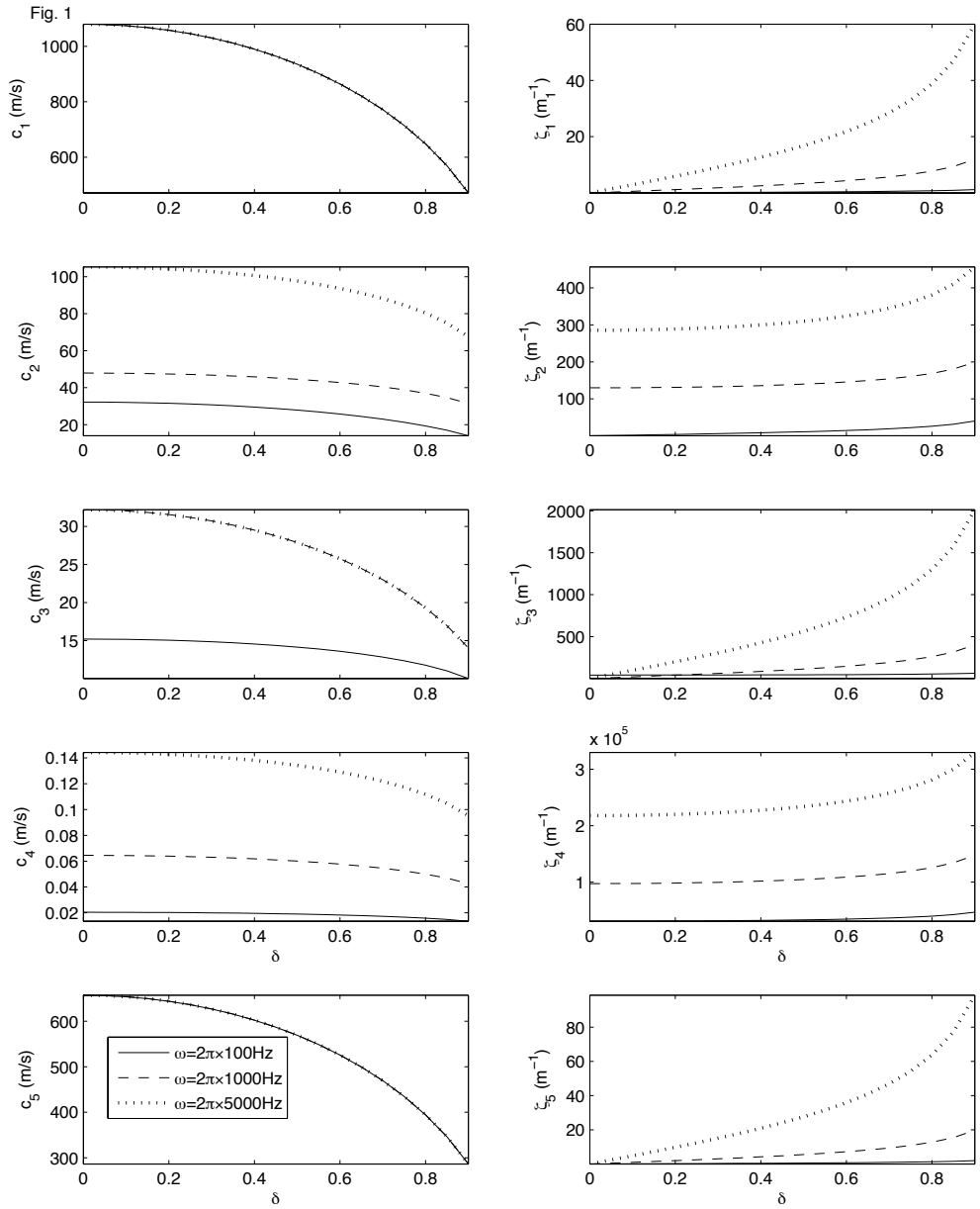

Figure 1 Phase velocities $(c_j, j = 1,2,3,4)$ and attenuation coefficients $(\zeta_j, j = 1,2,3,4)$ of P_1, P_2, P_3, P_4, S waves respectively; variations with inhomogeneity parameter (δ) and frequency (ω); $\alpha_f = 0.01$, $\sigma = 0.5$.

Effect of volume fraction of fractures

For three different values of volume fraction of fractures $\alpha_f = 0.01, 0.02, 0.03$, the variations of phase velocities and attenuation coefficients of the P_1, P_2, P_3, P_4 and S waves with $\delta \in [0,1)$ are as shown in Fig. 3. Except $\omega/2\pi = 0.1\text{kHz}$ and $\sigma = 0.2$, the values of other parameters are unchanged. Clearly, the velocity of the three longitudinal waves (i.e. P_1, P_2, P_3) increases with the increase of volume fraction of fractures whereas velocity of fast longitudinal wave (i.e. P_1) decreases with the increase of volume

Fig. 2

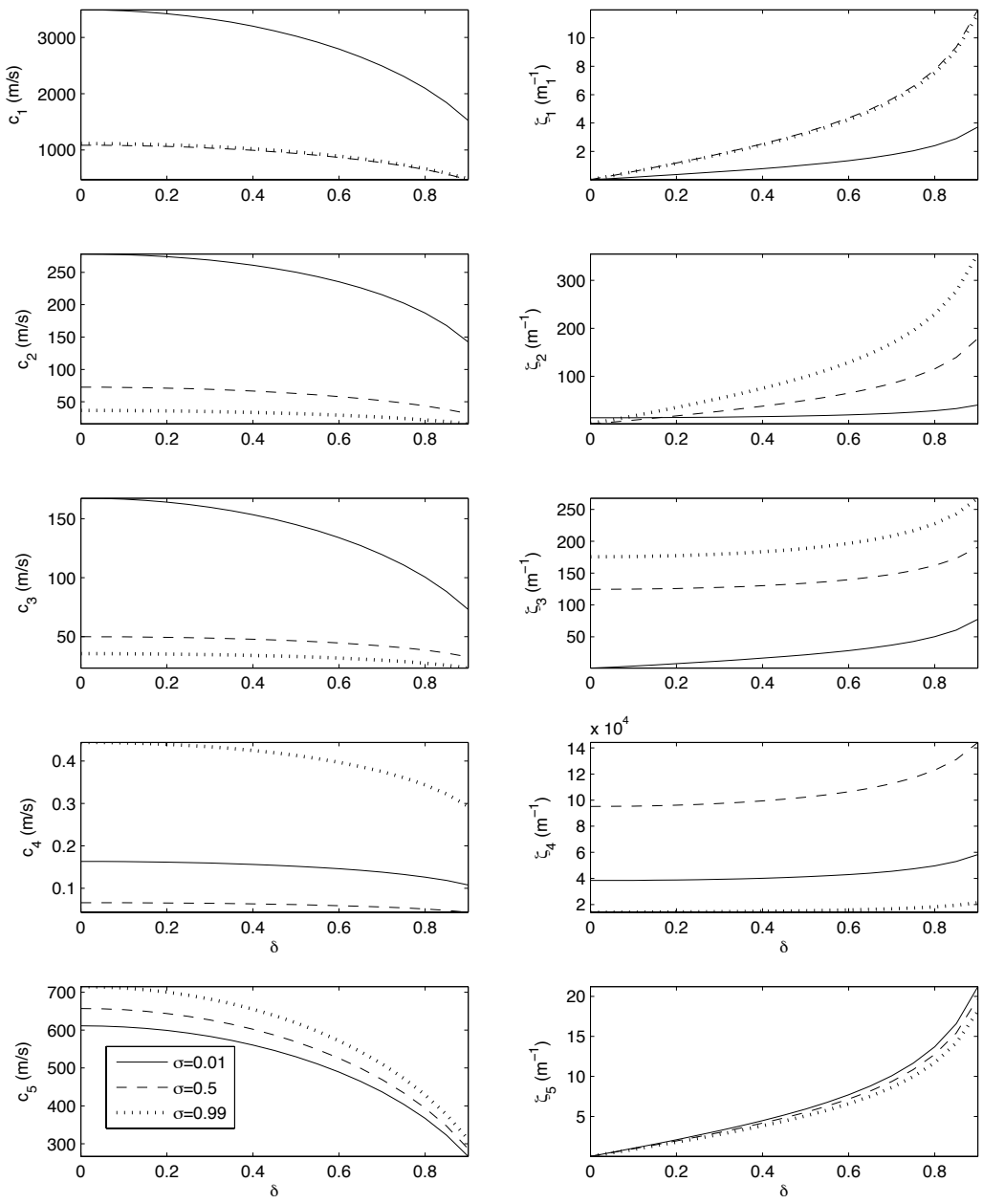

Figure 2 Phase velocities $(c_j, j = 1,2,3,4)$ and attenuation coefficients $(\zeta_j, j = 1,2,3,4)$ of P_1, P_2, P_3, P_4, S waves respectively; variations with inhomogeneity parameter (δ) and gas saturation (σ); $\alpha_f = 0.02, \omega/2\pi = 1kHz$.

fraction of fractures. However, the volume fraction of fractures shows no effect on the velocity and attenuation of faster shear wave (i.e. S). It is quite evident that the variations of the attenuation coefficient of a longitudinal wave with volume fraction of fractures appear nearly opposite to the variations in its velocity.

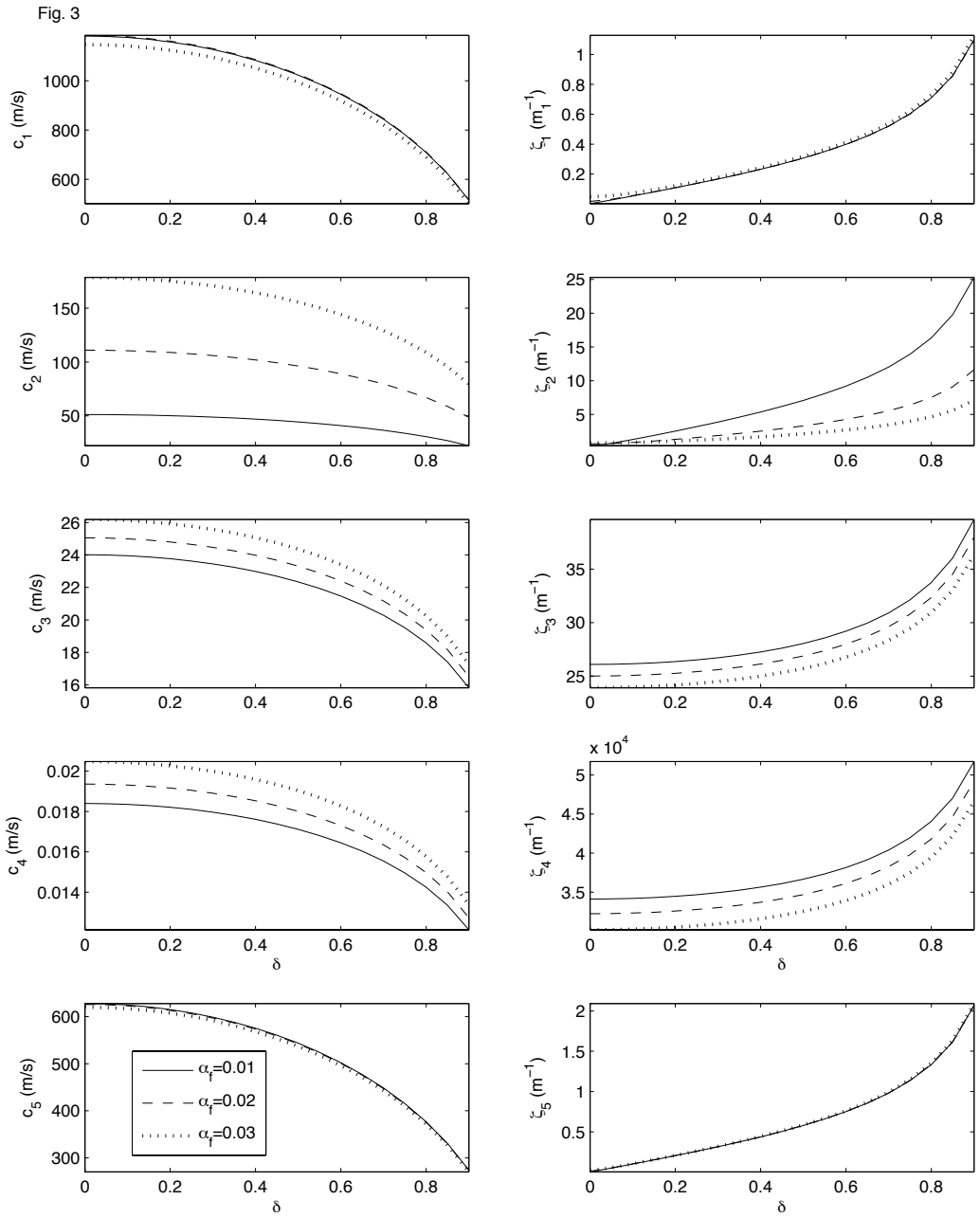

Figure 3 Phase velocities $(c_j, j = 1, 2, 3, 4)$ and attenuation coefficients $(\zeta_j, j = 1, 2, 3, 4)$ of P_1, P_2, P_3, P_4, S waves respectively; variations with inhomogeneity parameter (δ) and volume fraction of fractures (α_f); $\omega/2\pi = 0.1$ kHz, $\sigma = 0.2$.

Effect of inhomogeneity parameter

The variations of phase velocities and attenuation coefficients of the P_1, P_2, P_3, P_4 and S waves with $\delta \in (0, 1)$ are exhibited in Fig. 4 for three different values of $\delta = 0, 0.5, 0.9$. Values chosen for other parameters are unchanged except $\omega/2\pi = 0.1\text{kHz}$ and $\alpha_f = 0.02$. Increase of gas share seems to have a quiet significant effect of the velocities and attenuation coefficients of all the lon-

gitudinal waves (i.e., P_1, P_2, P_3, P_4). However, effect of gas share is observed very little on the velocity and attenuation coefficient of lone shear wave.

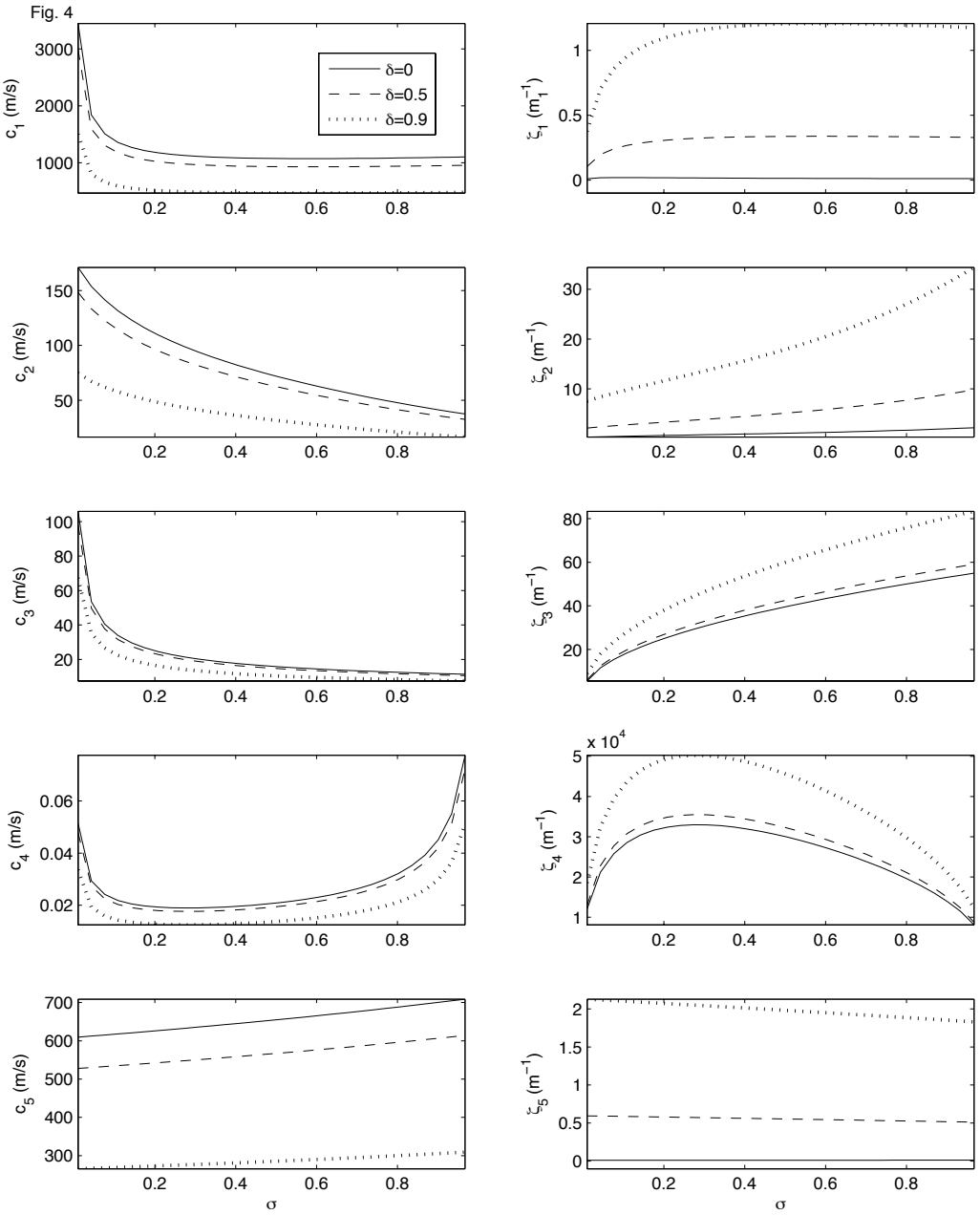

Figure 4 Phase velocities $(c_j, j = 1,2,3,4)$ and attenuation coefficients $(\zeta_j, j = 1,2,3,4)$ of P_1, P_2, P_3, P_4, S waves respectively; variations with gas saturation (σ) and inhomogeneity parameter (δ); $\omega/2\pi = 0.1$ kHz, $\alpha_f = 0.2$.

5.3 Reflection coefficients

The energy matrix defined in subsection 4.4 is calculated for a given value of incident angle θ varying from 0 to 90^0. For the present study, the incidence is considered of only two main waves,

i.e. P_1 and S. The low-frequency propagation is considered with circular frequency of 5kHz. The energy shares $E_{11}, E_{22}, E_{33}, E_{44}, E_{55}, E_{IR}$ and E_{RR} are computed and conservation of incident energy is ensured for

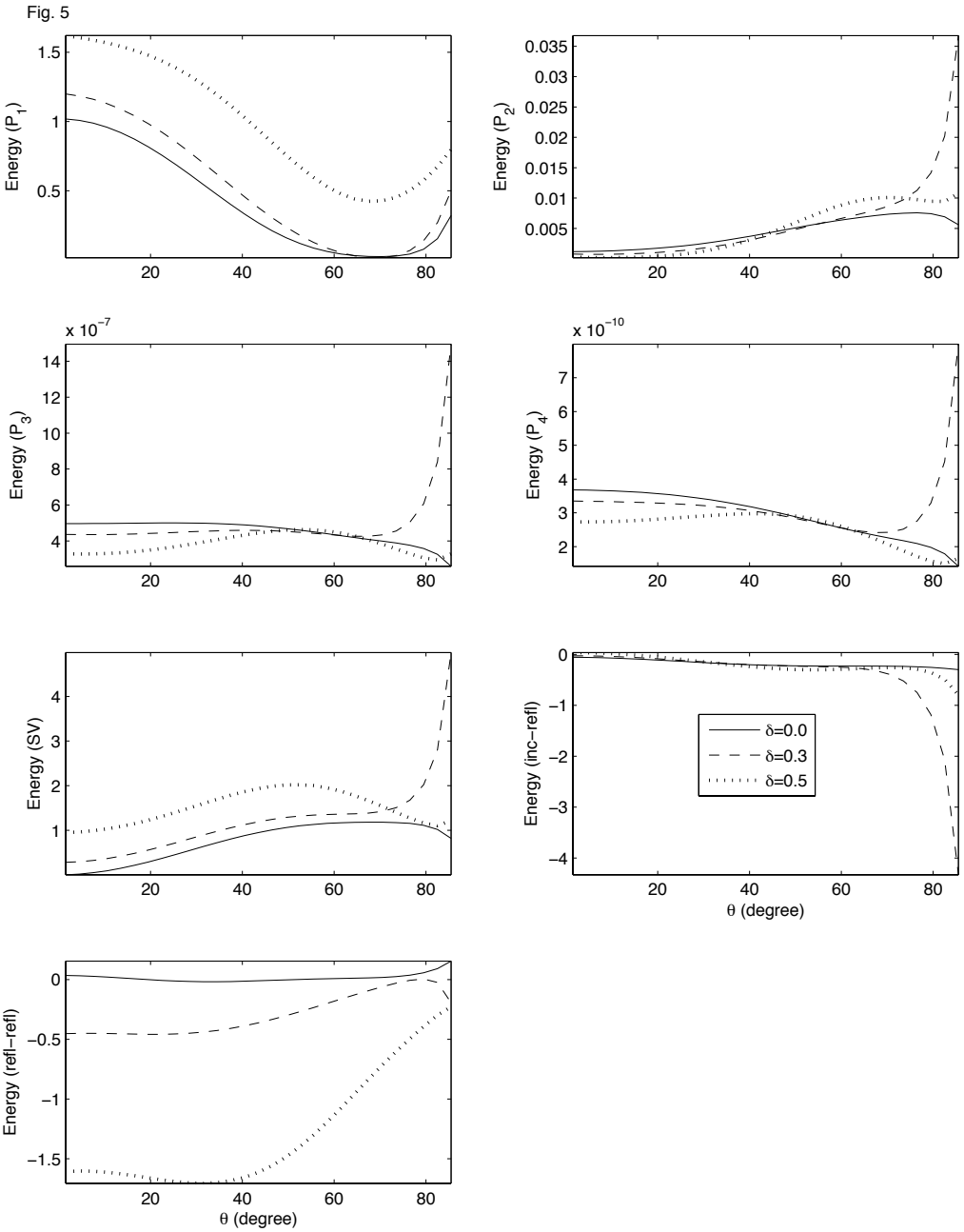

Figure 5 Energy shares of reflected (P_1, P_2, P_3, P_4, S) waves, incident wave and reflected waves interaction and interaction among reflected waves; variations with incident direction (θ) and inhomogeneity parameter (δ); $\omega/2\pi = 1\text{kHz}, \sigma = 0.02, \alpha_f = 0.01$.; incident P_1 wave.

each incidence. The $E_{11}, E_{22}, E_{33}, E_{44}$ and E_{55} denote the reflection coefficients for the reflected

P_1, P_2, P_3, P_4 and S waves, respectively. The variations of energy shares of reflected waves and interaction energies (E_{IR}, E_{RR}) with incident angle are shown in figures 5 to 8 (for incident P_1 wave) and in figures 9 to 12 (for incident S wave). The detailed discussion on figures is as follows.

The Fig. 5 exhibits the energy variations for three values (i.e. 0, 0.3, 0.5) of inhomogeneity parameter δ. Values chosen for other parameters are $\omega/2\pi = 1\text{kHz}, \sigma = 0.02, \alpha_f = 0.01$. It is noted that homogeneous propagation means almost no interaction of waves. In general, the presence of wave inhomogeneity strengthens the reflected waves with extra energy coming from the interaction (interference) of inhomogeneous waves present in the medium. It is quite evident that the energy shares of two slower longitudinal (P_3, P_4) waves are negligible. Further, the reflected (P_1, S) waves get more stronger with the increase of inhomogeneity strength of incident wave. Near the normal incidence, for any δ, reflected P_1 waves have larger energy shares. On the other hand, at grazing incidence, for any δ, only reflected S wave has a significant energy share. Negative sign of interaction energy implies the travel of energy towards the interface.

The Fig. 6 exhibits the energy variations for three values (i.e., 0.01, 0.02, 0.03) of volume fraction of fractures (i.e. α_f). Values chosen for other parameters are $\omega/2\pi = 1\text{kHz}, \sigma = 0.5, \delta = 0.2$. It is quite evident that the reflected (P_1, P_2, S) waves get more stronger with the increase of volume fraction of fractures. Near the normal incidence, for any α_f, reflected P_1 waves have larger energy shares. On the other hand, at grazing incidence, for any α_f, only reflected S wave has a significant energy share. From the energy shares of reflected waves, it is crystal clear that existence of the two slower longitudinal (i.e. P_3 and P_4) waves is namesake. A significant effect of volume fraction change is noticed on the interaction energies (E_{IR}, E_{RR}).

The Fig. 7 exhibits the energy variations for three different values (i.e., 0.01, 0.5, 0.99) of gas saturation (i.e., σ). Values chosen for other parameters are $\omega/2\pi = 1\text{kHz}, \alpha_f = 0.01, \delta = 0.2$. From the plots, it is quite evident that the significant energy shares of P_2 wave, particularly for $\sigma = 0.01$. It was also noticed that P_2, P_3 and P_3 waves are weakest when pore space is shared equally by two fluids. This implies that little gas share of gas in pores is more important for the existence of slower P waves then all gas or all liquid in pores. For the incidence below 17^0, the reflected P_1 wave strengthens with the increase of gas share in pores and beyond 17^0, the reflected P_1 wave weaken with the increase of gas share in pores, up to the incidence 43^0. Further, it is noticed that for the incidence below 43^0, the reflected S wave strengthens with the increase of gas share in pores and beyond 64^0, the reflected S wave weaken a lot with the increase of gas share in pores. A significant effect of saturating pore-fluid is noticed on the variations of interaction energies (i.e., E_{IR}, E_{RR}).

The variations of the energy shares with the incident direction are shown in Fig. 8, for three different frequencies i.e., $\omega/2\pi = 0.1, 1, 5\text{kHz}$. Values chosen for other parameters are $\sigma = 0.5, \alpha_f = 0.02, \delta = 0.2$. From the plots, it is noticed that a little effect of frequency change is observed on the energy shares of reflected P_1, P_2 and S waves. The effect of frequency is observed mainly for reflected P_3, P_4 waves and interaction energy (E_{RR}).

For the incidence of the S wave, energy partition at the surface is presented in Fig. 9 for three values (i.e., 0, 0.1, 0.2) of inhomogeneity parameter δ. Values chosen for other parameters are $\omega/2\pi = 1\text{kHz}, \sigma = 0.5, \alpha_f = 0.01$. The zero value of δ denotes the incidence of homogenous wave

Fig. 6

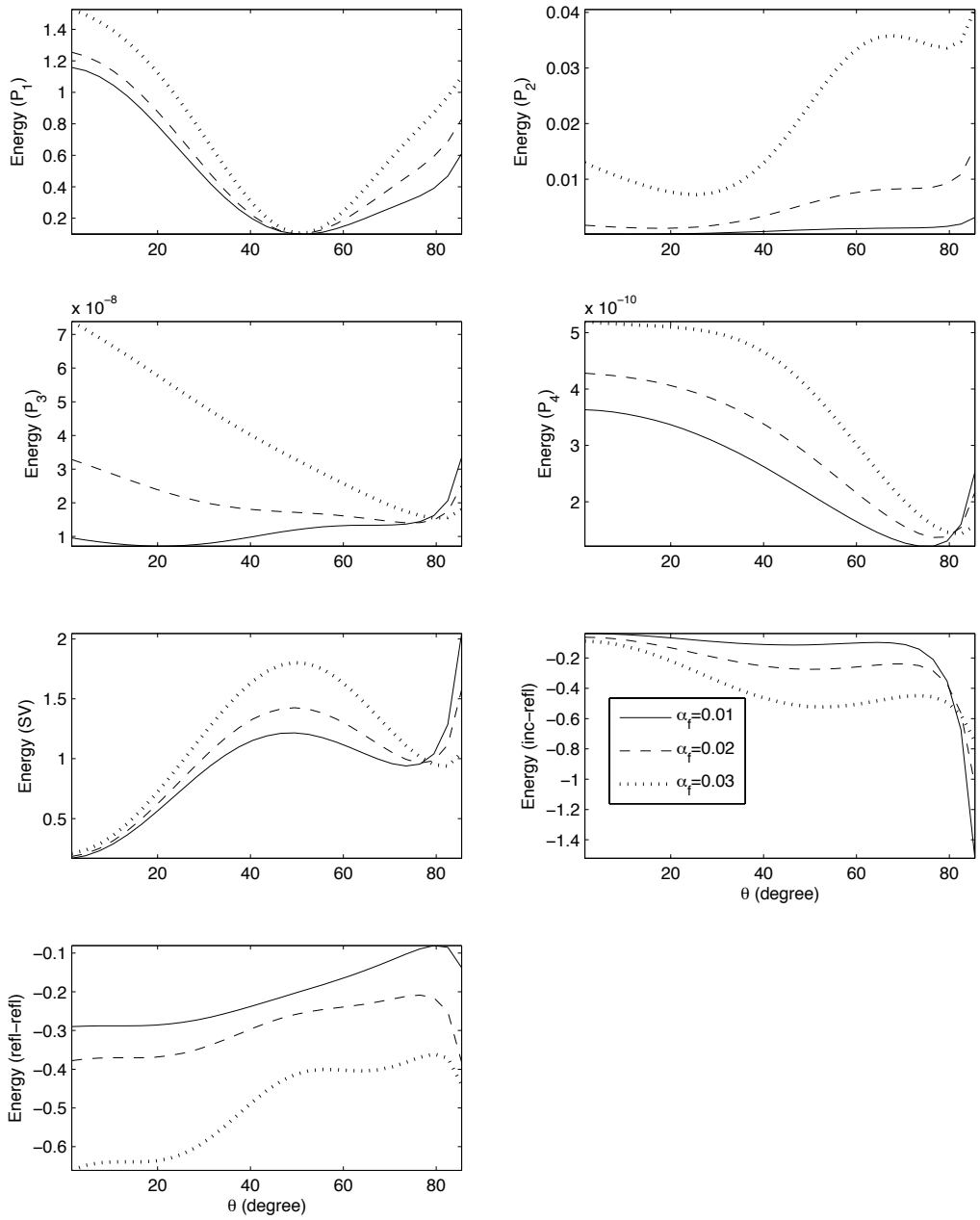

Figure 6 Energy shares of reflected (P_1, P_2, P_3, P_4, S) waves, incident wave and reflected waves interaction and interaction among reflected waves; variations with incident direction (θ) and volume fraction of fractures (α_f); $\omega/2\pi = 1\text{kHz}$, $\sigma = 0.5$, $\delta = 0.2$.; incident P_1 wave.

and a critical angle for reflected P_1 wave is around 40^0. Except near this critical incidence, more inhomogeneity of incident wave results in stronger reflected waves as well as excessive interaction. The energy shares are much larger near the grazing incidence. The reflection coefficients of P_3 and

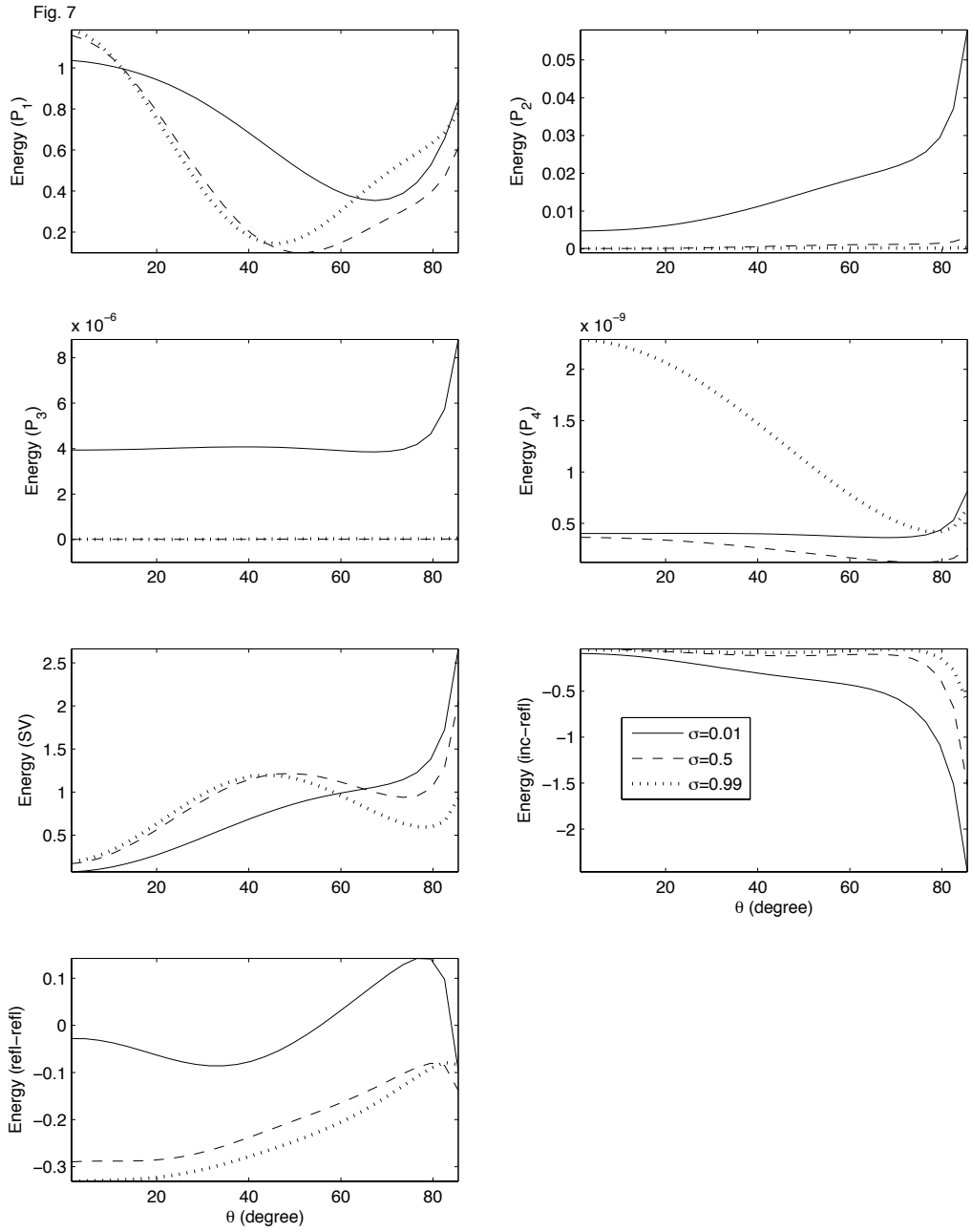

Figure 7 Energy shares of reflected (P_1, P_2, P_3, P_4, S) waves, incident wave and reflected waves interaction and interaction among reflected waves; variations with incident direction (θ) and gas saturation (σ); $\omega/2\pi = 1$kHz, $\alpha_f = 0.01$, $\delta = 0.2$.; incident P_1 wave.

P_4 waves are negligible. Further, it is quite evident that beyond critical incidence inhomogeneous propagation of waves is occurred for $\delta = 0$.

Fig. 10 exhibits the variations of the energy shares with the incident direction for three different values (i.e., 0.01, 0.02, 0.03) of volume fraction of fractures (i.e., α_f). Values chosen for other parameters are $\omega/2\pi = 1$kHz, $\sigma = 0.5, \delta = 0.2$. From the plots, it is noticed that the energy shares of all the

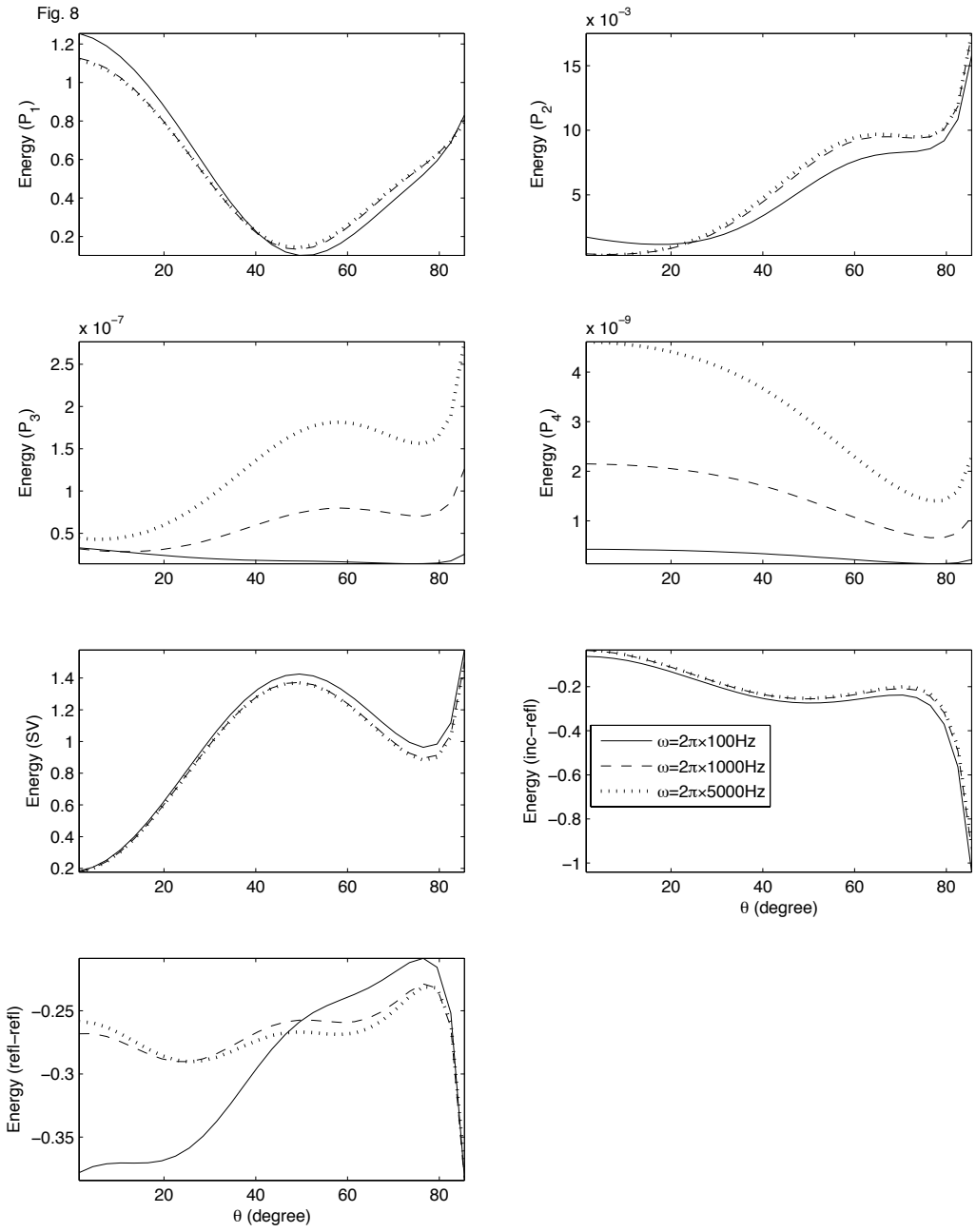

Figure 8 Energy shares of reflected (P_1, P_2, P_3, P_4, S) waves, incident wave and reflected waves interaction and interaction among reflected waves; variations with incident direction (θ) and frequency (ω);$\sigma = 0.5, \alpha_f = 0.02, \delta = 0.2.$; incident P_1 wave.

the reflected waves, except P_2 wave are decreases with the increase of volume fraction of fractures, near the grazing incidence. It is quite evident that beyond 40^0, for any α_f, the reflected P_2 wave have significant energy shares. Therefore, out of slower P waves, only P_2 wave is significant. For the incidence below 37^0, the energy shares of reflected P_1 wave decreases with the increase of

α_f and after that it start increasing with the increase of α_f. Then, beyond 67^0, it again decreases with the

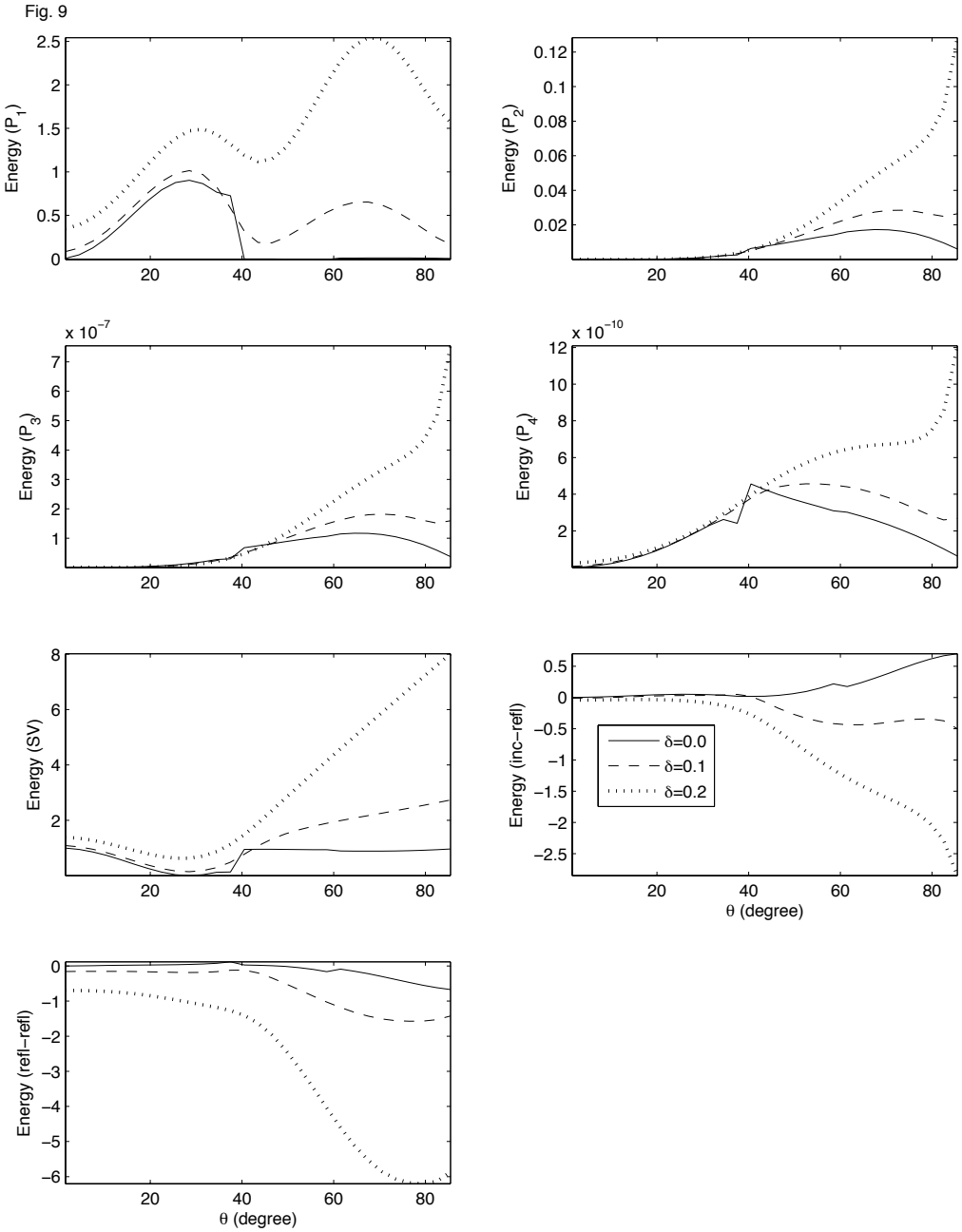

Figure 9 Energy shares of reflected (P_1, P_2, P_3, P_4, S) waves, incident wave and reflected waves interaction and interaction among reflected waves; variations with incident direction (θ) and inhomogeneity parameter (δ); $\omega/2\pi = 1\text{kHz}$, $\sigma = 0.02, \alpha_f = 0.01$.; incident S wave.

increase of α_f. A noticeable effect of volume fraction of fractures is observed on the energy shares of all the reflected waves and interaction energies.

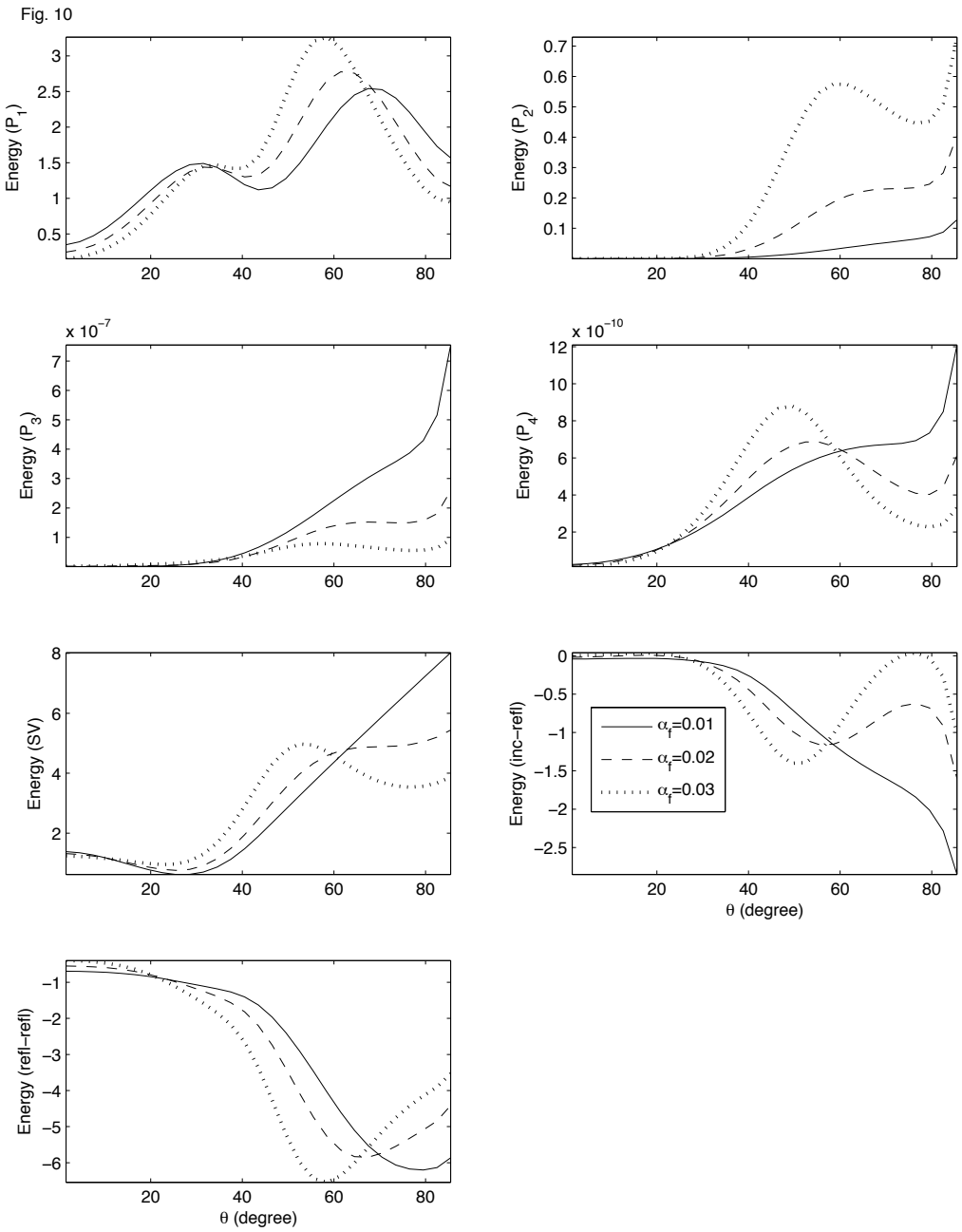

Figure 10 Energy shares of reflected (P_1, P_2, P_3, P_4, S) waves, incident wave and reflected waves interaction and interaction among reflected waves; variations with incident direction (θ) and volume fraction of fractures (α_f); $\omega/2\pi = 1$kHz, $\sigma = 0.5$, $\delta = 0.2$.; incident S wave.

Fig. 11 exhibits the variations of the energy shares with the incident direction for three different values (i.e., 0.01, 0.5, 0.99) of gas saturation (i.e., σ). Values chosen for other parameters are $\omega/2\pi = 1$kHz, $\alpha_f = 0.01$, $\delta = 0.2$. It is quite evident that near grazing incidence, for any value of

σ, the energy shares of reflected S wave dominates over other reflected waves. A significant energy

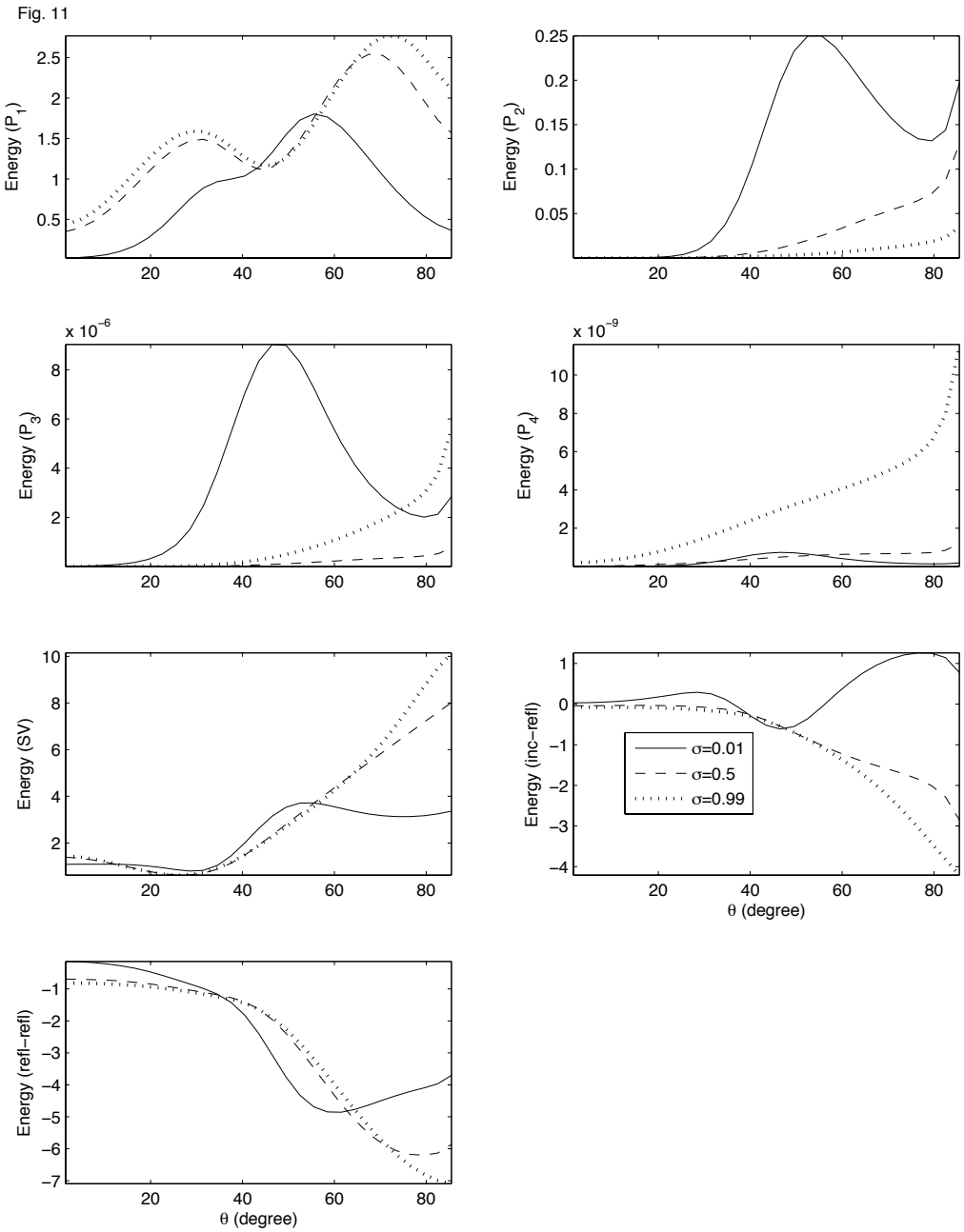

Figure 11 Energy shares of reflected (P_1, P_2, P_3, P_4, S) waves, incident wave and reflected waves interaction and interaction among reflected waves; variations with incident direction (θ) and gas saturation (σ); $\omega/2\pi = 1$kHz, $\alpha_f = 0.01$, $\delta = 0.2$.; incident S wave.

shares of reflected P_2 wave is observed, particularly for $\sigma = 0.01$. A noticeable effect of gas shares is observed on the energy shares of all the reflected waves and interaction energies.

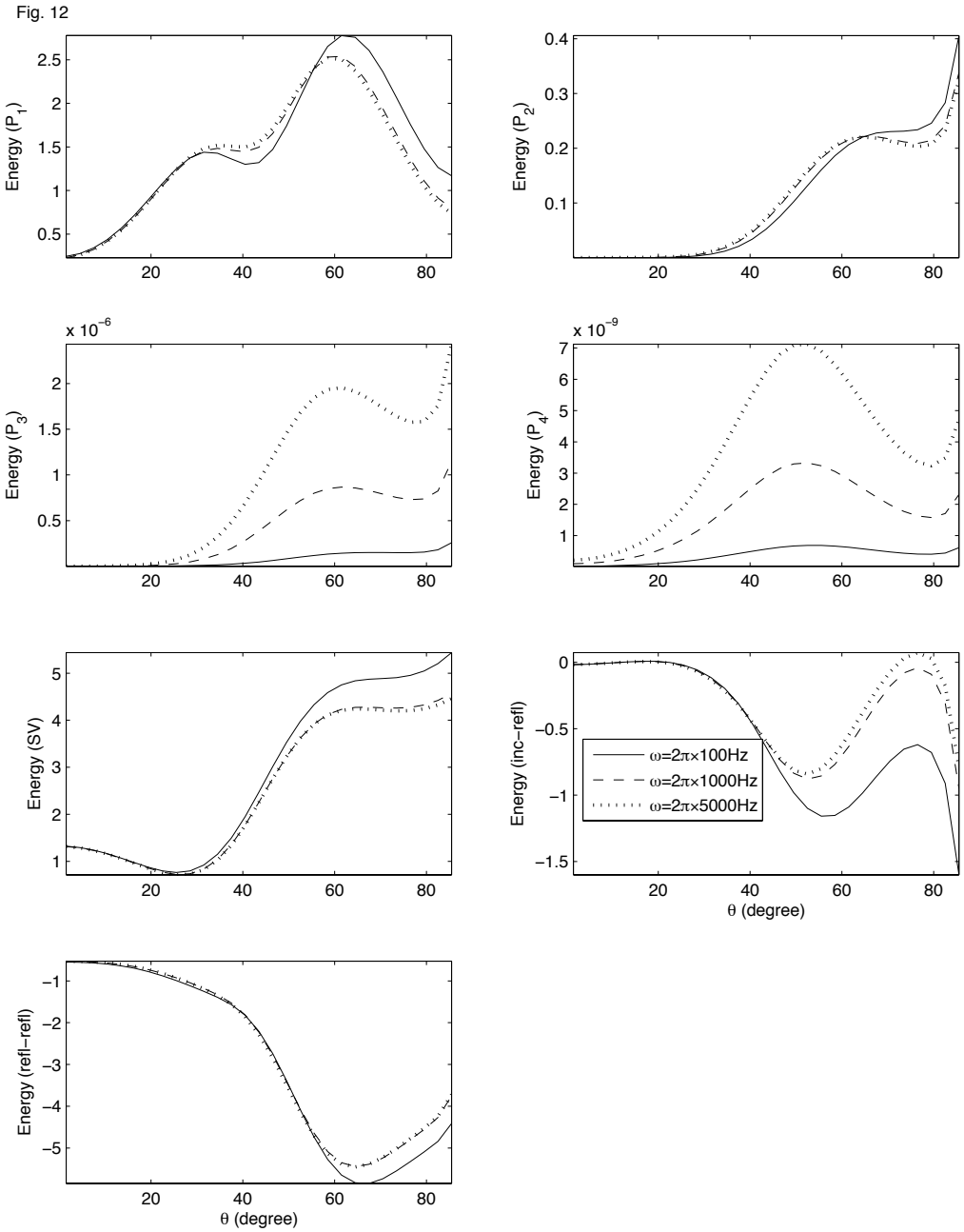

Figure 12 Energy shares of reflected (P_1, P_2, P_3, P_4, S) waves, incident wave and reflected waves interaction and interaction among reflected waves; variations with incident direction (θ) and frequency (ω); $\sigma = 0.5, \alpha_f = 0.02, \delta = 0.2.$; incident S wave.

The variations of the energy shares with the incident direction are shown in Fig. 12, for three different frequencies i.e., $\omega/2\pi = 0.1, 1, 5\text{kHz}$. Values chosen for other parameters are $\sigma = 0.5, \alpha_f = 0.02, \delta = 0.2$. Similar to the case on incident P_1 wave in Fig. 8, a little effect of frequency change is observed on the energy shares of reflected P_1, P_2 and S waves. The effect of frequency is observed mainly for reflected P_3, P_4 waves and interaction energy (E_{RR}).

6 CONCLUDING REMARKS

The work presented studies the inhomogeneous propagation of five attenuated (four dilatational and one shear) waves in a fractured porous solid. The fractured porous medium is dissipative due to the presence of viscous fluids in primary pores as well as secondary pores. The five attenuated waves in this dissipative medium are identified with complex velocities, which are resolved to calculate their phase velocities and attenuation coefficients for the general inhomogeneous propagation defined through a finite non-dimensional parameter. The variable gas share in pores enables to represent the pore saturation from almost all liquid to all gas. Reflection phenomenon is studied for incidence of only two main waves, that is P_1 and S. The changes in reflection energy coefficients are analyzed for a particular numerical model with variations in gas share in pores, frequency, volume fraction of fractures and inhomogeneity of incident wave. Some interesting observations from the numerical example may be important and hence are explained as follows.

- The phase velocities of all the waves may reduces to half with the change in propagation from homogeneous to evanescent. Attenuation increases with frequency as well as inhomogeneity. That means, the homogeneous waves may travel faster but cannot represent the wave motion with a larger attenuation. Moreover, a slower wave attenuates more in dissipative medium.
- Any change in frequency may not affect the phase velocity of two faster (P_1, S) waves.
- The increase of gas share increases the phase velocity of S wave whereas longitudinal waves except one (P_1) travel faster when the pore space is filled only with liquid.
- The increase of volume fraction of fractures (i.e. α_f) decreases the phase velocity of faster P_1 wave whereas phase velocity of other slower longitudinal waves increases with the increase of α_f. However, the effect of α_f is not observed on the phase velocity and attenuation of S wave.
- The variations of the phase velocity of a longitudinal wave with, frequency as well as volume fraction of fractures appear nearly opposite to the variations in its attenuation coefficient.
- The variations of the phase velocity of a wave with inhomogeneity appear nearly opposite to the variations in its attenuation coefficient. Moreover, the attenuation of two main waves is attributed more to the inhomogeneous propagation than the presence or increase of gas share in pores.
- For the considered numerical model, critical angle is observed only for reflected P_1 wave resulting from the incidence of the S wave, particularly for $\delta = 0$.
- For the incidence of $P_1(S)$ waves, out of slower P waves, only P_2 wave is significant. However, slower P_3 and P_4 waves are just negligible.
- An increase of volume fraction of fractures may strengthen the reflected P_1 wave from the near-normal incidence of P_1 wave. However, for incidence near-grazing, an increase of volume fraction of fractures may strengthen the reflected P_1 and P_2 waves whereas reflected P_3, P_4 and S waves may weaken.

- At the normal incidence of S wave, the change of volume fraction of fractures may have negligible effect on the energy shares of all reflected waves except P_1 wave. While at the grazing incidence of S wave, an increase of volume fraction of fractures may weaken the reflected P_1, P_2, P_3, P_4 and S waves whereas reflected P_2 wave may strengthen.
- The effect of inhomogeneity, volume fraction of fractures, frequency and gas shares in pores on energy partition is observed for all the reflected waves.
- Conservation of the incident energy is obtained for the presence of interaction energies due to the interference of incident wave and reflected waves. This certifies the correctness of all the analytic derivations which form the complete procedure.

References

Achenbach, J. D., 1973. Wave Propagation in Elastic Solids. 1st Edition, North-Holland Publishing, Amsterdam.

Aifantis, E. C., 1977. Introducing a multiporous medium. Development in Mechanics 8, 209-211.

Aifantis, E. C., 1979. On the response of fractured rocks. Development in Mechanics 8, 249-253.

Aifantis, E. C., 1980. On the problem of diffusion in solids. Acta Mechanica 37, 265-296.

Ainslie, M. A., and Burns, P. W., 1995. Energy-conserving reflection and transmission coefficients for a solid-solid boundary. Journal of the Acoustical Society of America 98, 2836-2840.

Arora, A., Tomar, S. K., 2010. Seismic reflection from an interface between an elastic solid and a fractured porous medium with partial saturation. Transport in Porous Media 85(2), 375-396.

Auriault, J. L., Boutin, C., 1993. Deformable porous media with double porosity. Transport in Porous Media 10, 153-159.

Bai, M., Elsworth, D., Roegiers, J. C., 1993. Modelling of naturally fractured reservoirs using deformation dependant flow mechanism. International Journal of Rock Mechanics and Mining Sciences and Geomechanics 30(7), 1185-1191.

Barenblatt, G. I., Zheltov, I. P., Kochina, I. N., 1960. Basic concepts in the theory of seepage of homogeneous liquids in fractured rocks (strata). Prikladnaya Matematika i Mekhanika 24(5), 1286-1303.

Berryman, J. G., 1980. Confirmation of Biot's theory. Applied Physics Letters 37(4), 382-384.

Berryman, J.G., Wang, H.F., 1995. The elastic coefficients of double-porous models for fluid transport in jointed rock. Journal of Geophysical Research: Solid Earth 100, 24611-24627.

Berryman, J.G., Wang, H.F., 2000. Elastic wave propagation and attenuation in a double-porosity dual-permeability media. International Journal of Rock Mechanics and Mining Science 37, 63-78.

Beskos, D.E., Aifantis, E.C., 1986. On the theory of consolidation with double porosity-II. International Journal of Engineering Science 24, 1697-1716.

Biot, M. A., 1956. Theory of propagation of elastic waves in a fluid saturated porous solid, I. Low-frequency range, II. Higher frequency range. Journal of the Acoustical Society of America 28(2), 168-191.

Biot, M. A., 1962. Mechanics of deformation and acoustic propagation in porous media. Journal of Applied Physics 33, 1482-1498.

Biot, M. A., 1962. Generalized theory of acoustic propagation in porous dissipative media. Journal of the Acoustical Society of America 34(5), 1254-1264.

Borcherdt, R.D., 1982. Reflection-refraction of general P and type-I S waves in elastic and anelastic solids. Geophysical Journal of Royal Astronomical Society 70, 621-638.

Carcione, J. M., Cavallini, F., 1995. Forbidden directions for inhomogeneous pure shear waves in dissipative anisotropic media. Geophysics 60, 522-530.

Deresiewicz, H., Skalak, R., 1963. On uniqueness in dynamic poroelasticity. Bulletin of the Seismological Society of America 53, 783-789.

Duguid, J. O., Lee, P.C.Y., 1977. Flow in fractured porous media. Water Resources Research 13(3), 558-566.

Krebes, E. S., 1983. The viscoelastic reflection/ transmission problem: two special cases. Bulletin of Seismological Society of America 73, 1673-1683.

Krebes, E. S., Le, L. H. T., 1994. Inhomogeneous plane waves and cylindrical waves in anisotropic anelastic media. Journal of Geophysical Research 99, 23899-23919.

Khaled, M. Y., Beskos, D. E., Aifantis, E. C., 1984. On the theory of consolidation with double porosity-III. A finite element formulation. International Journal for Numerical and Analytical Methods in Geomechanics 8, 101-123.

Khalili, N., 2003. Coupling effects in double porosity media with deformable matrix. Geophysical Research Letters 30(22), 2153. doi:10.1029/2003GL018544.

Khalili, N., Valliappan, S., 1996. Unified theory of flow and deformation in double porous media. European Journal of Mechanics A/Solids 15(2), 321-336.

Khalili-Naghadeh, N., Valliappan, S., 1991. Flow through fractured porous media with deformable matrix: Implicit formulation. Water Resources Research 27(7), 1703-1709.

Khalili, N., Valliappan, S., Wan, C. F., 1999. Consolidation of fractured clays. Geotechnique, 49(1), 75-89.

Kumar, M., Saini, R., 2012. Reflection and refraction of attenuated waves at boundary of elastic solid and porous solid saturated with two immiscible viscous fluids. Applied Mathematics and Mechanics 33(6), 2012, 797-816.

Kumar, M., Sharma, M. D., 2013. Reflection and transmission of attenuated waves at the boundary between two dissimilar poroelastic solids saturated with two immiscible viscous fluids. Geophysical Prospecting 61(5), 1035-1055.

Loret, B., Rizzi, E., 1999. Strain localization in fluid saturated anisotropic elastic-plastic porous media with double porosity. Journal of the Mechanics and Physics of Solids 47, 503-530.

Plona, T. J., 1980. Observation of a second bulk compressional wave in a porous medium at ultrasonic frequencies. Applied Physics Letters 36(4), 259-261.

Sams, M.S., Neep, J.P., Worthington, M.H., King, M. S., 1997. The measurements of velocity dispersion and frequency-dependent intrinsic attenuation in sedimentary rocks. Geophysics 62, 1456-1464.

Sharma, M. D., 2008. Propagation of inhomogeneous plane waves in viscoelastic anisotropic media. Acta Mechanica 200, 145-154.

Sharma, M. D., Kumar, M., 2011. Reflection of attenuated waves at the surface of a porous solid saturated with two immiscible viscous fluids. Geophysical Journal International 184, 371-384.

Sharma, M. D., Saini, R., 2012. Wave propagation in porous solid containing liquid filled bound pores and two-phase fluid in connected pores. European Journal of Mechanics A/Solids 36, 53-65.

Tuncay, K., Corapcioglu, M.Y., 1996a. Wave propagation in fractured porous media. Transport in Porous Media 23, 237-258.

Tuncay, K., Corapcioglu, M.Y., 1996b. Body waves in fractured porous media saturated by two immiscible newtonian fluids. Transport in Porous Media 23, 259-273.

Tuncay, K., Corapcioglu, M.Y., 1997. Wave propagation in poroelastic media saturated by two fluids. Journal of Applied Mechanics 64, 313-319.

Valliappan, S., Khalili-Naghadeh, N., 1990. Flow through fractured porous media with deformable matrix. International Journal of Numerical Method in Engineering Science 29, 1079-1094.

Wang, H. F., Berryman, J. G., 1996. On constitutive equations and effective stress principles for deformable, double-porosity media. Water Resources Research 32(12), 3621-3622.

Warren, J. B., Root, P. J., 1963. The behaviour of naturally fractured reservoirs. Society of Petroleum Engineers Journal 3, 245-255.

Wilson, R. K., Aifantis, E. C., 1982. On the theory of consolidation with double porosity-II. International Journal of Engineering Science 20(9), 1009-1035.

Wilson, R. K., Aifantis, E. C., 1984. A double porosity model for acoustic wave propagation in fractured-porous rock. International Journal of Engineering Science 22, 1209-1217.

Appendix

$$a_{11}^{*} = a_{11} - \frac{2}{3}G_{fr}, \qquad a_{11}^{**} = a_{11} + \frac{1}{3}G_{fr},$$

$$\begin{aligned}
a_{11} = \Big[&\{\alpha_s\alpha_f(\alpha_p + E_1K_{fr}) - \alpha_pE_3K_2'(1 + E_2K_{fr}) - E_1E_3K_{fr}K_2'(1 - \alpha_f)\}\alpha_sD_2K_{fr}K_s \\
&- \{\alpha_s\alpha_f\alpha_p \\
&+ D_2\alpha_pE_3\Big[-(1 - \alpha_f)K_2'^2\sigma - P_{cap}'\sigma(1 - \sigma)\big(K_2'(1 - \sigma\alpha_f) + \sigma\alpha_fK_1'\big) \\
&- K_1'K_2'\big(1 - \sigma(1 - \alpha_f)\big)\Big]\}K_{fr}K_s\Big]/D_3,
\end{aligned}$$

$$\begin{aligned}
a_{12} = \Big[&\{\alpha_s\alpha_f(\alpha_p + E_1K_{fr}) - \alpha_pE_3K_2'(1 + E_2K_{fr}) - E_1E_3K_{fr}K_2'(1 - \alpha_f)\}(K_2' \\
&+ P_{cap}'\sigma(1 - \sigma))\alpha_1K_sK_1'\Big]/D_3,
\end{aligned}$$

$$\begin{aligned}
a_{13} = \Big[&\{\alpha_s\alpha_f(\alpha_p + E_1K_{fr}) - \alpha_pE_3K_2'(1 + E_2K_{fr}) - E_1E_3K_{fr}K_2'(1 - \alpha_f)\}(K_2' \\
&+ P_{cap}'\sigma(1 - \sigma))\alpha_2K_sK_2'\Big]/D_3,
\end{aligned}$$

$$a_{14} = -\Big[\{-\alpha_s\alpha_p(\alpha_f + E_2K_{fr})D_2 + D_1(\alpha_p + K_{fr}(E_1(1 - \alpha_f) + \alpha_pE_2))\}\alpha_fK_sK_2'\Big]/D_3,$$

$$\begin{aligned}
a_{21} = \Big[&\Big(-\alpha_s\alpha_f + E_3K_2'(1 + E_2K_{fr})\Big)\Big(K_2' + P_{cap}'\sigma(1 - \sigma)\Big)\alpha_1\alpha_sK_sK_1' \\
&+ (\alpha_s\alpha_f - \alpha_fE_3K_s - E_3K_2' + \alpha_fE_2K_2')(K_2' + P_{cap}'\sigma(1 - \sigma))\alpha_1K_{fr}K_1')\Big]/D_3,
\end{aligned}$$

$$\begin{aligned}
a_{22} = \Big[&\Big\{-\sigma K_s\Big(\alpha_f\alpha_p\alpha_s - \alpha_pE_3K_2'(1 + E_2K_{fr})\Big)\Big(K_2' + P_{cap}'(1 - \sigma)\Big) \\
&- K_2'P_{cap}'\sigma(1 - \sigma)^2(-\alpha_s\alpha_f(\alpha_p + E_1K_{fr}) + \alpha_pE_3K_2'(1 + E_2K_{fr}) \\
&+ E_1E_3K_{fr}(K_2'(1 - \alpha_f) + \alpha_fK_s))\Big\}\alpha_1K_1'\Big]/D_3,
\end{aligned}$$

$$\begin{aligned}
a_{23} = \Big[&\Big\{(\alpha_pE_3K_2'(1 + E_2K_{fr}) - \alpha_s\alpha_f(\alpha_p + E_1K_{fr}) + E_1E_3K_{fr}(K_2'(1 - \alpha_f) \\
&+ \alpha_fK_s))P_{cap}'\sigma(1 - \sigma) + K_s\Big(-\alpha_f\alpha_p\alpha_s + \alpha_pE_3K_2'(1 + E_2K_{fr})\Big)\Big\}\sigma(1 \\
&- \sigma)\alpha_pK_1'K_2'\Big]/D_3,
\end{aligned}$$

$$a_{24} = \Big[\{(-\alpha_s\alpha_f - \alpha_sE_2K_{fr} + E_3K_s + E_2E_3K_sK_{fr})(K_2' + P_{cap}'\sigma(1 - \sigma))\}\alpha_1\alpha_fK_1'K_2'\Big]/D_3,$$

$$a_{31} = \Big[\Big(-\alpha_s\alpha_f + E_3K_2'\big(1+E_2K_{fr}\big)\Big)\Big(K_1' + P_{cap}'\sigma(1-\sigma)\Big)\alpha_2\alpha_sK_sK_2' + \big(\alpha_s\alpha_f - \alpha_fE_3K_s - E_3K_2' + \alpha_fE_3K_2'\big)(K_1' + P_{cap}'\sigma(1-\sigma))\alpha_2K_{fr}K_2')\Big]/D_3,$$

$$a_{32} = \Big[\Big\{(\alpha_sE_3K_2'\big(1+E_2K_{fr}\big) - \alpha_s\alpha_f\big(\alpha_p + E_1K_{fr}\big) + E_1E_3K_{fr}(K_2'\big(1-\alpha_f\big) + \alpha_fK_s))P_{cap}'\sigma(1-\sigma) + K_s\Big(-\alpha_f\alpha_p\alpha_s + \alpha_pE_3K_2'\big(1+E_2K_{fr}\big)\Big)\Big\}\sigma(1-\sigma)\alpha_pK_1'K_2'\Big]/D_3,$$

$$a_{33} = \Big[-K_s(1-\sigma)\Big(\alpha_f\alpha_p\alpha_s - \alpha_pE_3K_2'\big(1+E_2K_{fr}\big)\Big)\big(K_1' + \sigma P_{cap}'\big)\alpha_1K_1' - K_1'P_{cap}'\sigma^2(1-\sigma)(-\alpha_f\alpha_s\big(\alpha_p + E_1K_{fr}\big) + \alpha_pE_3K_2'\big(1+E_2K_{fr}\big) + E_1E_3K_{fr}(K_2'\big(1-\alpha_f\big) + \alpha_fK_s)))\alpha_sK_2'\Big]/D_3,$$

$$a_{34} = \Big[\big\{\big(-\alpha_s\alpha_f - \alpha_sE_2K_{fr} + E_3K_s + E_2E_3K_sK_{fr}\big)(K_1' + P_{cap}'\sigma(1-\sigma))\big\}\alpha_2\alpha_fK_2'^2\Big]/D_3,$$

$$a_{41} = \Big[-\big(\alpha_s\alpha_fE_1E_3D_1K_{fr}K_sK_2'\big) + (E_3K_sD_2 - E_3D_1)\alpha_f\alpha_pK_{fr}K_2'\Big]/D_3,$$

$$a_{42} = \Big[-\alpha_1\alpha_fE_1E_3K_{fr}K_sK_1'K_2'(K_2' + P_{cap}'\sigma(1-\sigma))\Big]/D_3,$$

$$a_{43} = \Big[-\alpha_2\alpha_fE_1E_3K_{fr}K_sK_2'^2(K_1' + P_{cap}'\sigma(1-\sigma))\Big]/D_3,$$

$$a_{44} = \Big[-\big\{(E_1E_3K_{fr}K_s - \alpha_s\alpha_p - \alpha_sE_1K_{fr})\alpha_fD_1 + \alpha_s\alpha_f\alpha_pK_sD_2\big\}\alpha_fK_2'\Big]/D_3,$$

where

$$\alpha_p = 1 - \alpha_s - \alpha_f,$$
$$D_1 = K_1'K_2' + P_{cap}'\sigma(1-\sigma)(\sigma K_1' + (1-\sigma)K_2'),$$

$$D_2 = (1-\sigma)\big(K_1' + \sigma P_{cap}'\big) + \sigma K_2',$$
$$D_3 = \big[\big\{\alpha_s\alpha_f\big(\alpha_p + E_1K_{fr}\big) - \alpha_pE_3K_2'\big(1+E_2K_{fr}\big) - E_1E_3K_{fr}(K_2'\big(1-\alpha_f\big) + \alpha_fK_s)\big\}D_1 + \big\{-\alpha_f\alpha_p\alpha_s + \alpha_pE_3K_2'\big(1+E_2K_{fr}\big)\big\}K_sD_2\big],$$
$$E_1 = \frac{1}{K_s} - \frac{1-\alpha_f}{K_{fr}^m}, \quad E_2 = \frac{1-\alpha_f}{K_{fr}^m} - \frac{1}{K_{fr}}, \quad E_3 = F\left(\frac{\alpha_s}{K_s} - \frac{\alpha_s^2}{K_{fr}}\right),$$

where K_1', K_2', K_s, K_{fr} and K_{fr}^m denote the bulk modulus of non-wetting fluid phase, wetting fluid phase, solid grains, fractured porous medium and non-fractured porous medium, respectively. α_i is the volume fraction of phase i. σ is the fraction of non-wetting fluid saturation in the composite medium. F is a material parameter associated with the change in volume fraction of fractures P_{cap}' is equivalent bulk modulus for macroscopic capillary pressure (Garg & Nayfeh 1986).